RSC Advances

PAPER

View Article Online
View Journal | View Issue

Cite this: *RSC Adv.*, 2025, **15**, 45233

Novel bakuchiol derivatives inhibit the migration and invasion of non-small cell lung cancer by suppressing epithelial-to-mesenchymal transition

Meng-Fan Xu,[a] Ke Zhong,[a] Jing Zhu,[a] Jie Chen,[a] Fang Liu,[ab] Feng Ding,[ab] Cheng-Zhu Wu*[ab] and Long Zhao *[ab]

Recently, bakuchiol and its derivatives have been widely investigated owing to their anticancer activity. However, there are few studies on the inhibition of epithelial–mesenchymal transition (EMT) by bakuchiol and its derivatives. Besides, thiosemicarbazones (TSCs) have also been demonstrated to exhibit potential EMT-inhibitory effects. Hence, the cytotoxic activity of novel bakuchiol derivatives containing thiosemicarbazone moieties was evaluated against two non-small lung cancer cell lines. Among them, compound **2f** demonstrated the highest activity, with IC_{50} values of 2.23 and 5.55 μM against PC9 and H1975 cells, respectively. Compound **2f** effectively suppresses tumor cell proliferation by inducing cell cycle arrest and promoting apoptosis. Additionally, various evidence after treatment with compound **2f** in PC9 cells, including the inhibition of migration and invasion, the enhancement of E-cadherin expression and reduction of vimentin levels, indicated the role of bakuchiol derivatives in inhibiting EMT. These findings suggest that bakuchiol derivatives could be positioned as potential candidates for cancer treatment.

Received 30th June 2025
Accepted 29th October 2025

DOI: 10.1039/d5ra04625d

rsc.li/rsc-advances

Introduction

EMT is a complex biological process that is crucial in various physiological and pathological contexts, such as embryonic development, wound healing, fibrosis, and cancer metastasis.[1] During EMT, epithelial cells undergo programmed changes, which enable them to lose their characteristic cell–cell adhesion and polarity and acquire mesenchymal-like properties, enhancing their ability to invade surrounding tissues and migrate to new locations.[2–4] In addition, these are accompanied by changes in epithelial cell markers, such as a decrease in cytokeratins and E-cadherin and increase in N-cadherin, vimentin and snail.[5,6] This transition allows epithelial cells to become more motile, invasive, and resistant to apoptosis, characteristics that are crucial for cancer cells to metastasize and spread to distant organs.[7] EMT is regulated by a complex network of signaling pathways and transcription factors, and its dysregulation has been implicated in the progression of various cancers.[8] Therefore, developing new compounds that can be used to suppress EMT is essential for developing targeted therapies to inhibit cancer metastasis and improve patient outcomes.

Non-small cell lung cancer (NSCLC) accounts for the majority of all lung cancers, which encompasses various subtypes, including adenocarcinoma, squamous cell carcinoma, and large cell carcinoma.[9,10] NSCLC typically originates from the epithelial cells lining the airways and is frequently linked to a history of smoking or exposure to carcinogens.[11,12] In the context of NSCLC, EMT has been implicated in promoting the invasiveness and metastatic potential of cancer cells.[13,14]

Bakuchiol, a natural compound found in the seeds of the *Psoralea corylifolia* plant, has been demonstrated to play an important role in preventing the development of lung cancer cells.[15–18] Studies have shown that by inducing apoptosis and cell cycle arrest, bakuchiol can effectively restrict the growth and spread of lung cancer cells.[15] Moreover, bakuchiol has shown antioxidant and anti-inflammatory properties, which could help in decreasing inflammation and oxidative stress linked to the development of cancer.[19–22] Additionally, bakuchiol has been found to inhibit the process of EMT in lung cancer cells.[16]

TSCs are a class of organic compounds that have gained attention for their potential application in anti-tumor.[23–27] TSCs have shown synergistic effects when combined with conventional chemotherapy drugs, enhancing their efficacy and reducing drug resistance.[28–32] Alternatively, TSCs function as iron chelators, exerting anti-tumour and anti-metastatic effects by upregulating Ndrg-1. Ndrg-1 suppresses TGF-β-induced EMT in tumour cells by stabilizing E-cadherin/β-catenin adhesion complexes and enhancing intercellular adhesion.[33] In 2020, Liu

[a]*School of Pharmacy, Bengbu Medical University, Bengbu, Anhui, China. E-mail: wuchengzhu0611@bbmu.edu.cn; zhaolong@bbmu.edu.cn*

[b]*Anhui Province Biochemical Pharmaceutical Engineering Technology Research Center, Bengbu, Anhui, China*

et al. reported the synthesis of a series of TSC-based lead compounds, which exhibited excellent antiproliferative activity against MGC803 cells and inhibited EMT.[34] Consequently, by employing the molecular hybridization strategy, we hope to link TSCs with bakuchiol *via* a condensation reaction and further explore their application in the treatment of NSCLC (Fig. 1). In this work, a series of novel bakuchiol derivatives were designed and synthesized to enhance the anti-cancer activity of bakuchiol. Their cytotoxicity was evaluated against two non-small cell lung cancer cell lines. Furthermore, we found that the bakuchiol derivatives exhibited good inhibition of migration and invasion, which was manifested by inhibiting EMT.

Results and discussion

Chemistry

As depicted in Scheme 1, bakuchiol derivatives (**2a–2t**) were designed and synthesized *via* the condensation reaction between 2-formyl-bakuchiol **1** and different commercially available substituted thiosemicarbazides. Notably, a series of alkyl, substituted benzene and heterocyclic rings were considered in this study, showcasing the versatility and potential of these derivatives in further applications. The chemical structures of the bakuchiol derivatives were characterized using ^{1}H-NMR, ^{13}C-NMR and HR-ESI-MS (see SI).

Biological evaluation

***In vitro* cytotoxicity of bakuchiol derivatives.** All the synthesized compounds (**1** and **2a–2t**) were investigated for their cytotoxicity *in vitro* against two human lung cancer cell lines (PC9 and H1975) preliminary using the MTT method. Alkannin and bakuchiol have structural similarities including phenolic hydroxyl groups, conjugated systems with aromatic structures, and hydrophobic side chains, all of which suggest that they may have similar anti-tumor activity, and thus alkannin was employed as a positive control (Table 1). A series of analogues of compound **2a** were synthesized and evaluated for their cytotoxicity. Firstly, compounds **2b–2c** and **2m**, bearing simple alkyl substituents on the side chain of TSCs, exhibited significantly reduced cytotoxic activity. This suggests that hydrophobic substituents may be detrimental to increased cytotoxicity. Compared with compound **2a**, compounds **2d–2e**, **2q–2r** and **2t**, containing heterocyclic substituted alkyl groups, displayed a non-significant increase in cytotoxicity. Further, the compounds with benzene rings as the substituent group in TSCs were employed to investigate their cytotoxic activity in PC9 and H1975 cells (compounds **2f–2l**). The IC_{50} value of compound **2f** against the human lung cancer cell lines (PC9 and H1975) was 2.23 and 5.55 μM, respectively, indicating their excellent cytotoxic activity. Compared with bakuchiol, compound **2f** was 2.12-fold and 2.13-fold more cytotoxic to PC9

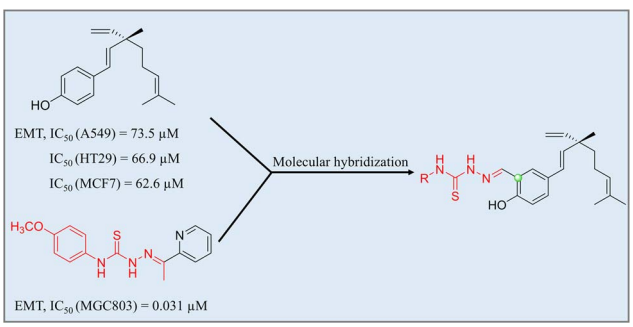

Fig. 1 Molecular hybridization strategy for the design of bakuchiol derivatives.[16,32,34]

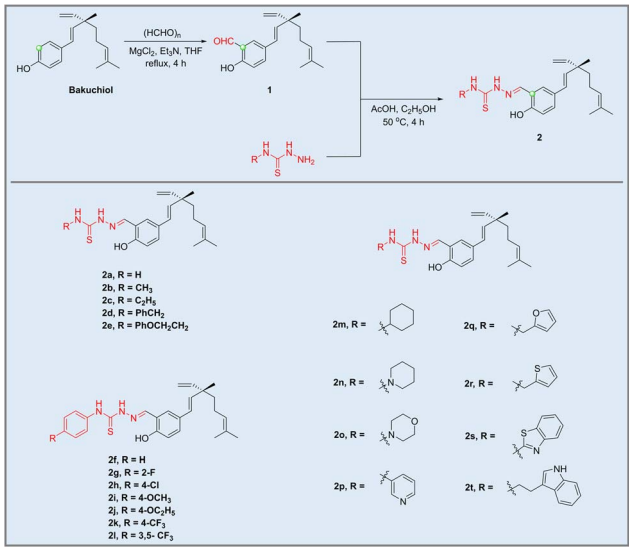

Scheme 1 Synthetic pathway for bakuchiol derivatives.

Table 1 Cytotoxic activity of compounds **1**, **2a–2t**, bakuchiol, and alkannin (IC_{50}, μM, and 48 h)

Compound	PC9	H1975
1	22.42	13.77
2a	18.56	15.75
2b	38.12	>100
2c	14.84	15.84
2d	4.94	13.08
2e	14.16	11.55
2f	2.23	5.55
2g	8.57	34.44
2h	8.75	12.16
2i	7.46	18.15
2j	10.12	20.43
2k	6.88	37.80
2l	16.39	18.28
2m	28.02	25.96
2n	30.21	67.41
2o	20.48	34.67
2p	10.80	12.56
2q	11.14	14.02
2r	17.49	15.41
2s	78.88	>100
2t	11.35	16.75
Bakuchiol	4.73	11.82
Alkannin[a]	5.62	5.27

[a] Positive control.

and H1975 cells, respectively. Compared with gefitinib, compound **2f** has relatively weak cytotoxicity against PC9 cells (gefitinib, 0.014 μM IC_{50}, 72 h)[35] and strong cytotoxicity against H1975 cells (gefitinib, 6.5 μM IC_{50}, 72 h).[36] Furthermore, heterocyclic and aromatic heterocyclic substituents also were investigated, and the cytotoxic activity of the compound did not improve. Moreover, compound **2f** exhibited low cytotoxicity toward normal mouse hepatocytes (Aml-12 cells), with an IC_{50} value of 19.00 μM, in contrast to its significant cytotoxicity action against PC9 and H1975 cells (Table 2). Thus, based on its superior cytotoxic profile, compound **2f** was selected for further investigation.

Anti-proliferative activity of compound 2f

The remarkable findings presented in Fig. 2 unveil the compelling concentration- and time-dependent anti-proliferative potential of compound **2f** against the PC9 and H1975 human lung cancer cell lines. Notably, this study also revealed the varying sensitivity of these two cell lines to the growth-inhibiting effects of compound **2f**, with PC9 cells emerging as particularly susceptible to its remarkable action.

Effects of compound 2f on cell cycle phase arrest

The effects of compound **2f** on cell cycle phase arrest in PC9 and H1975 cells were evaluated at its IC_{50} by flow cytometry. After treatment for 24 h with compound **2f**, the cells were harvested and analyzed by flow cytometry. The results indicated that compound **2f** can prolong the S phase and shorten the G1 and G2 phases in PC9 cells compared with the control group. The cell cycle phase arrest of compound **2f** in H1975 cells is different from that in PC9 cells, where compound **2f** prolongs the G1 phase and shortens the S and G2 phases. The above-mentioned results suggested that compound **2f** induces cell cycle phase arrest in PC9 and H1975 cells (Fig. 3).

Compound 2f-induced apoptosis in PC9 cells

To functionally confirm the engagement of apoptotic pathways, we utilized a chemical inhibition strategy with z-VAD-FMK. The cell viability of PC9 cells was rescued after co-treatment with compound **2f** and z-VAD-FMK, which demonstrates that the suppression of proliferation is contingent on the induction of apoptosis (Fig. 4A). To further elucidate the role of reactive oxygen species (ROS) in cell death, *N*-acetylcysteine (NAC), a known ROS scavenger, was employed to assess the intracellular ROS levels. As depicted in Fig. 4B, treatment with compound **2f** (4 μM) alone resulted in a 126% increase in intracellular ROS. However, this elevation was significantly reduced to 107% upon co-treatment with NAC ($p < 0.05$).

Table 2 Cytotoxic activity of compound **2f** on Aml-12 cells (IC_{50}, μM, 72 h)

Compound	AmI-12
2f	19.00 ± 1.46
Alkannin	14.50 ± 2.08

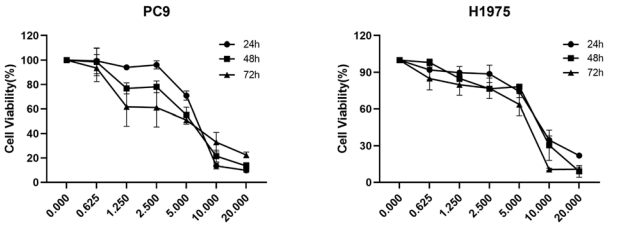

Fig. 2 Anti-proliferative activities of compound **2f** in NSCLC cells: the viabilities of the PC9 and H1975 human lung cancer cells treated with various concentrations (0, 0.625, 1.25, 2.5, 5, 10, and 20 μM) of compound **2f** for 24, 48, and 72 h.

Furthermore, NAC exhibited a protective effect against compound **2f**-induced cell death in PC9 cells (Fig. 4C, $p < 0.01$), supporting the involvement of ROS in the cytotoxic mechanism. Apoptosis was quantified *via* annexin V/PI dual staining, followed by flow cytometric analysis. Treatment of PC9 cells with compound **2f** for 24 h resulted in a dose-dependent increase in apoptotic cell death. As illustrated in Fig. 4D, the percentage of apoptotic cells reached 17.2%, 19.0%, and 20.6% at concentrations of 2, 4, and 8 μM, respectively. These results indicated that compound **2f** induced apoptosis in the PC9 cells.

Compound 2f inhibits the migration and invasion of PC9 cells

Given that most cases of lung cancer are detected only in the final stages of the disease, high mortality is strongly associated with metastasis.[37] Migration and invasion and are critical processes involved in tumour metastasis, with cancer cells breaking away from the primary tumour site and spreading to distant organs. Understanding how compounds can affect these processes can help in developing targeted therapies to inhibit metastasis and improve patient outcomes.[38] Hence, we examined the impact of compound **2f** on the capabilities of migration and invasion in PC9 cells. The migration and invasion ability of

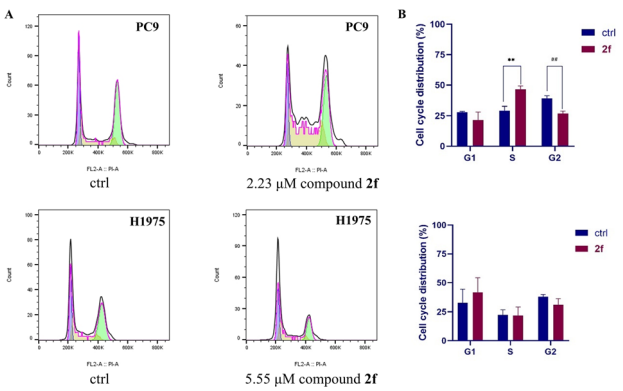

Fig. 3 (A) Effects of compound **2f** on the cell cycle phase arrest in PC9 and H1975 cells. Cells were treated for 24 h with compound **2f** (2.23 μM and 5.55 μM). Cells were then fixed and stained with PI to analyse their DNA content by flow cytometry. (B) Percentage of PC9 and H1975 cells in different phases of the cell cycle. Data are presented as the mean ± SD from three independent experiments. $^{**}p < 0.01$ and $^{\#\#}p < 0.01$ *versus* the control group.

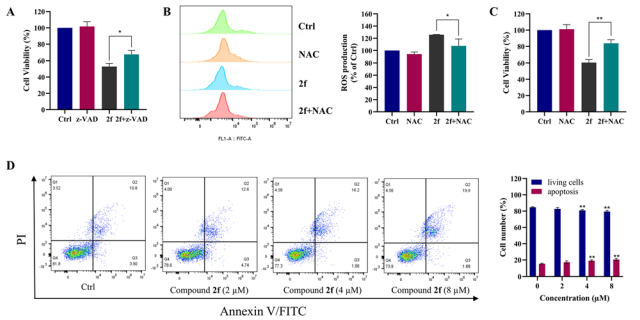

Fig. 4 Compound **2f** induced apoptosis in PC9 cells. (A) Cell viability following treatment with compound **2f** (4 μM) for 24 h alone or pre-treatment with z-VAD-FMK (20 μM) as measured by the MTT assay. (B) Intracellular ROS level analysis following treatment with compound **2f** (4 μM) or pre-treatment with NAC (20 μM). (C) Cell viability following treatment with **2f** (4 μM) for 24 h alone or pre-treatment with NAC as measured by the MTT assay. (D) Flow cytometric analysis of cell death treated with different concentrations (0, 2, 4, and 8 μM) of compound **2f** using annexin V/PI dual staining. Related histograms for living and apoptotic cells are displayed. *$p < 0.05$ and **$p < 0.01$ *vs.* ctrl cells.

the PC9 cells was reduced as the concentration of compound **2f** increased. In conclusion, compound **2f** has concentration-dependent ability to dramatically suppress PC9 cell migration and invasion (Fig. 5A, B, 63S and 64S). Moreover, higher levels of MMP2 and MMP9 have been linked to greater cell invasion and migratory capacities.[39] The results of western blotting demonstrated the down-regulation of MMP2 and MMP9 expression, supporting the proposal that compound **2f** might prevent PC9 cells from migrating and invading. Furthermore, to assess the potential impact of compound **2f** on EMT, western blotting also was performed to analyse the expression of mesenchymal markers (vimentin) and epithelial markers (E-cadherin). We found that the expression of E-cadherin was upregulated and the expression of vimentin was downregulated after treatment with compound **2f** in PC9 cells. The findings demonstrated that compound **2f** successfully suppressed the EMT process of PC9 cells (Fig. 5C and D).

Compound 2f inhibits the migration and invasion of PC9 cells induced by TGF-β

Migration and invasion are closely linked to EMT because EMT is a process that enables epithelial cells to acquire migratory and invasive properties, allowing them to metastasize to distant sites in the body.[3,40,41] Besides, TGF-β, which is a key regulator of EMT, can induce EMT, promoting the migration and invasion of cancer cells in the stage of tumour progression. Therefore, following TGF-β induction, the inhibitory effects of bakuchiol derivatives on their migration and invasion were investigated, which are closely related with the effects of bakuchiol derivatives on EMT.[42,43]

We examined the effects of compound **2f** on the migration and invasion of PC9 cells induced by TGF-β. The migration and invasion ability of PC9 cells was significantly enhanced after induction with 30 ng per mL TGF-β. Compared with the control group, the enhancement amplitude of migration and invasion was 1.7-fold and 1.4-fold, respectively. The results indicated that TGF-β successfully induced the migration and invasion of PC9 cells. After treatment with compound **2f**, the migration and invasion ability of the PC9 cells was dramatically inhibited in a dose-dependent manner (Fig. 6A, B, S65 and S66). The above-mentioned data suggested that compound **2f** inhibited the migration and invasion of PC9 cells induced by TGF-β associated with EMT. To examine the impact of compound **2f** on EMT caused by TGF-β, we used western blotting to assess the E-cadherin expression levels. The findings demonstrated that following TGF-β stimulation, E-cadherin expression declined and compound **2f** restored the expression of E-cadherin. Finally, compound **2f** can reverse the TGF-β-induced EMT process (Fig. 6C and D).

In vivo antitumor efficacy and biosafety

To further assess the *in vivo* antitumor efficacy of compound **2f**, we established a Balb/c nude mouse model with subcutaneous PC9 tumours. When the size of the tumour reached 100 mm^3, the nude mice were randomly assigned to three groups, as

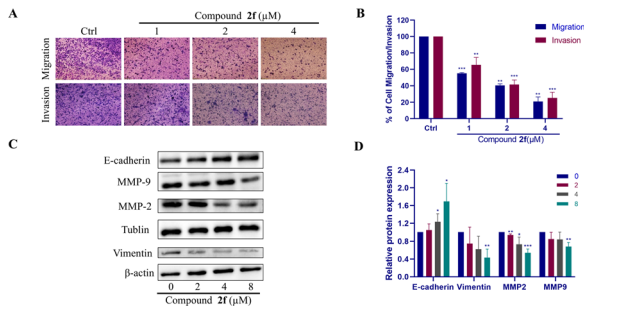

Fig. 5 (A) Cells treated with compound **2f** (0, 1, 2, and 4 μM) for 24 h. Representative photomicrographs of the membrane-associated cells stained with crystal violet. (B) Cell migration and invasion values quantified as the fold ratio of invaded cells ($n = 3$). (C) Western blotting analysis of the E-cadherin, vimentin, MMP2, and MMP9 protein levels. (D) Protein relative expression from western blotting quantified as the fold ratio ($n = 3$). *$p < 0.05$, **$p < 0.01$, and ***$p < 0.001$ *vs.* ctrl cells.

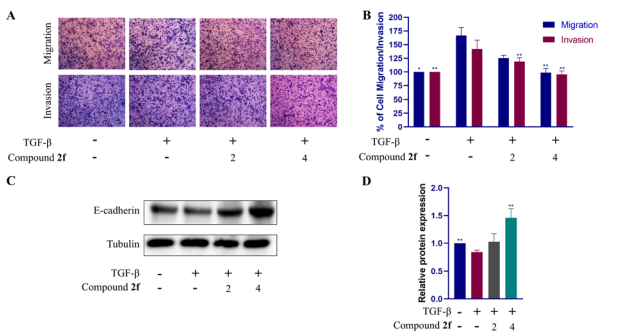

Fig. 6 (A) Cells treated with compound **2f** (0, 2, 4 μM), with or without 30 ng per mL TGF-β for 24 h. Representative photomicrographs of membrane-associated cells stained with crystal violet. (B) Cell migration and invasion values quantified as the fold ratio of invaded cells ($n = 3$). (C) Western blotting analysis of the E-cadherin levels. (D) Protein relative expression from western blotting quantified as the fold ratio ($n = 3$). *$p < 0.05$ and **$p < 0.01$ *vs.* TGF-β-treated cells.

follows: saline, DDP, and compound **2f**. Compared with the control group, compound **2f** showed a more obvious tumour inhibition effect and weaker weight change in the nude mice after three times intraperitoneal administration (Fig. 7C). After 18 days of treatment, all the nude mice were killed by neck removal to remove their tumours and organs. Compared with the control group, compound **2f** can effectively inhibit tumour growth and has less effect on the body weight of the nude mice. The DDP group also showed similar tumour suppression but had a higher impact on the body weight of the nude mice (Fig. 7A–D). The results of the histopathological examination showed that compound **2f** had no obvious damage to the organs of the nude mice (Fig. 7E). Then, we examined the expression of E-cadherin and vimentin in the xenografts by IHC. Similar to the results in the *in vitro* study, IHC analysis revealed that compound **2f** can effectively inhibit the progression of EMT, where the expression of E-cadherin significantly increased, while the expression of vimentin diminished (Fig. 7F). The above-mentioned result indicated that bakuchiol derivatives might reverse TGF-β-induced EMT by modulating the E-cadherin and vimentin levels. In conclusion, these findings revealed that compound **2f** has excellent anti-tumour activity *in vivo*.

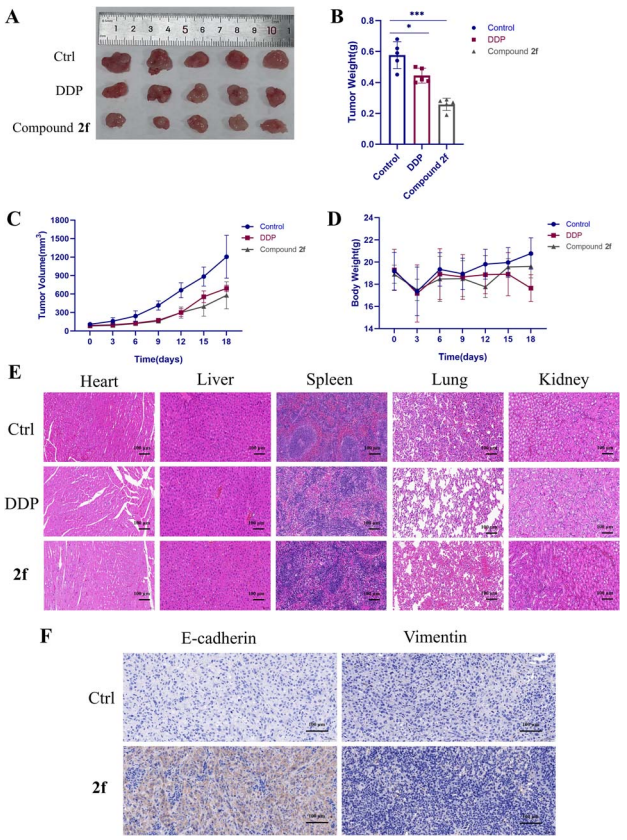

Fig. 7 (A) Tumour image at the end of the whole therapy period. (B) Tumour weight of mice after different treatments. (C) Growth curve of tumour volume during treatment with saline, DDP (2 mg kg^{-1}), and compound **2f** (20 mg kg^{-1}). (D) Body weight changes in mice after different treatments. (E) Histopathological examination (H&E) of the main organ sections removed from the tumour-bearing mice treated with saline, DDP, and compound **2f** (20 mg kg^{-1}). (F) Immunohistochemistry staining of E-cadherin and vimentin in xenograft tissues ($n = 3$). All data are presented as mean ± SD ($n = 5$). *$p < 0.05$; **$p < 0.01$; and ***$p < 0.001$ *vs.* ctrl.

Conclusions

In this study, we aimed to enhance the activity of bakuchiol derivatives through molecular hybridization. We successfully introduced TSCs with different substituents at the α-position of the hydroxyl group through Friedel–Crafts acylation and condensation reactions. A series of bakuchiol derivatives (**2a–2t**) containing thiosemicarbazone moieties were designed, synthesized and evaluated for their anti-cancer activities *in vitro* against two human lung cancer cell lines (PC9 and H1975 cells). The bakuchiol derivatives with benzene rings in TSCs exhibited better cytotoxicity compared with alkyl- and heterocyclic-substituted TSC bakuchiol derivatives. Especially, compound **2f** demonstrated significant inhibition of PC9 and H1975 cell proliferation *in vitro*, along with highly effective anti-tumour effects *in vivo*. Besides, histopathological assessment of major organs revealed no apparent treatment-related lesions following the administration of compound **2f**. Coupled with the absence of significant body weight loss, these findings suggest a favorable preliminary safety profile for compound **2f** at the tested doses. The cell cycle results also indicated that compound **2f** can cause cell cycle phase arrest. Moreover, in conjunction with its pro-apoptotic effects, these results suggest that compound **2f** exerts its antiproliferative activity through both cell cycle disruption and apoptosis induction. Compound **2f** significantly inhibited the invasion and migration of PC9 cells induced by TGF-β. Additionally, it was observed that compound **2f** suppressed EMT by regulating the expression of E-cadherin and vimentin. These findings suggest that bakuchiol derivatives have potential as anti-tumour agents in the discovery and development of anti-NSCLC drugs.

Experimental

Materials and characterization

All commercially available compounds were used without further purification. TLC plates and column chromatography silica gel (300–400 mesh) were purchased from Qingdao Haiyang Chemical Co. NMR spectra were recorded on a Bruker Avance II (300 MHz or 400 MHz) instrument. HRMS spectra were obtained using a Thermo Scientific LTQ Orbitrap XL mass spectrometer (Bruker, Bremerhaven, Germany).

General procedure for the synthesis of compound 1

To a solution of bakuchiol (3 g, 11.7 mmol) in anhydrous THF (18 mL), $MgCl_2$ (2.2 g, 23.4 mmol), $(HCHO)_n$ (1.1 g, 35.1 mmol) and Et_3N (3.2 mL, 23.4 mmol) were added, and the reaction was kept at 70 °C for 4 h. After the reaction was finished, the reaction was quenched with 10% hydrochloric acid solution. The product was extracted three times with ethyl acetate (30 mL). The organic layer was combined and dried over anhydrous

Na_2SO_4. Then, the solvent was removed under reduced pressure. The residue was purified by flash chromatography on silica gel to afford pure compound **1** using petroleum/ethyl acetate (30 : 1).

(*S*,*E*)-5-(3,7-Dimethyl-3-vinylocta-1,6-dien-1-yl)-2-hydroxybenzaldehyde (1). Yellow oil, yield 68%, purity ≥ 95% by HPLC. ^{1}H-NMR (300 MHz, DMSO-d_6) δ 10.73 (br, 1H, ArOH), 10.25 (s, 1H, CHO), 7.66 (s, 1H, ArH), 7.62 (dd, J = 8.4 Hz, 1H, ArH), 6.96 (d, J = 8.6 Hz, 1H, ArH), 6.28 (d, J = 16.4 Hz, 1H, CHC*H*), 6.16 (d, J = 16.4 Hz, 1H, C*H*CH), 5.90 (dd, J = 17.5 Hz, 1H, C*H*C(CH$_3$)$_2$), 5.10 (t, J = 10.5 Hz, 1H, CC*H*CH$_2$), 5.02 (dd, J = 10.5 Hz, 2H, CCHC*H*$_2$), 1.90 (m, 2H, CCH$_2$*CH*$_2$), 1.63 (s, 3H, C(*CH*$_3$)$_2$), 1.53 (s, 3H, C(*CH*$_3$)$_2$), 1.46 (m, 2H, C(*CH*$_2$)$_2$), 1.17 (s, 3H, C*CH*$_3$). ^{13}C-NMR (75 MHz, DMSO-d_6) δ 192.0 (CHO), 160.3 (C_{Ar}OH), 146.1 (C*C*HCH$_2$), 136.6 (C$_{Ar}$*C*HCH), 134.3 (C_{Ar}), 131.0 (*C*(CH$_3$)$_2$), 129.4 (C_{Ar}), 126.7 (C$_{Ar}$CH*C*H), 125.9 (C_{Ar}), 125.1 (*C*HC(CH$_3$)$_2$), 122.6 (C_{Ar}), 118.0 (C_{Ar}), 112.5 (CCH*C*H$_2$), 42.7 (C*C*H$_2$CH$_2$), 41.3 (*C*CH$_2$CH$_2$), 25.9 (C*C*H$_3$), 23.3 (C(*C*H$_3$)$_2$), 17.9 (C(*C*H$_3$)$_2$).

General procedure for the synthesis of compounds 2a–2t

To a solution of compound **1** (1.0 equiv.) and different substituted thiosemicarbazides (1.2 equiv.) in EtOH, acetic acid (0.01 equiv.) was added. The reaction was kept at room temperature for 4 h. When compound **1** was completely consumed, the reaction was quenched with aq $NaHCO_3$. The product was extracted three times with ethyl acetate (30 mL). The combined organic layer was dried over anhydrous Na_2SO_4 and the solvent was removed under reduced pressure. The residue was purified by flash chromatography on silica gel to afford pure compound **2** using petroleum/ethyl acetate.

2-((*E*)-5-((*S*,*E*)-3,7-Dimethyl-3-vinylocta-1,6-dien-1-yl)-2-hydroxybenzylidene)hydrazine-1-carbothioamide (2a). White solid, yield 95%, purity ≥ 95% by HPLC. ^{1}H-NMR (300 MHz, CDCl$_3$) δ 10.35 (s, 1H, CHNN*H*), 9.36 (s, 1H, –O*H*), 8.13 (s, 1H, C*H*NNH), 7.37 (dd, J = 8.6 Hz, 1H, ArH), 7.23 (d, J = 2.0 Hz, 1H, ArH), 6.93 (d, J = 8.5 Hz, 1H, ArH), 6.57 (s, 2H, N*H*$_2$), 6.24 (d, J = 16.3 Hz, 1H, CHC*H*), 6.09 (d, J = 16.3 Hz, 1H, C*H*CH), 5.88 (dd, J = 17.4 Hz, 1H, C*H*C(CH$_3$)$_2$), 5.14–4.98 (m, 3H, CC*H*CH$_2$), 1.95 (q, J = 7.5 Hz, 2H, CCH$_2$*CH*$_2$), 1.68 (s, 3H, C(*CH*$_3$)$_2$), 1.58 (s, 3H, C(*CH*$_3$)$_2$), 1.54–1.47 (m, 2H, C*CH*$_2$CH$_2$), 1.20 (s, 3H, C*CH*$_3$). ^{13}C NMR (101 MHz, CDCl$_3$) δ 177.40 (NNH*C*S), 156.51 (C_{Ar}OH), 148.63 (C*C*HCH$_2$), 145.61 (*C*HNNH), 137.12 (C$_{Ar}$*C*HCH), 131.45 (C_{Ar}), 130.59 (*C*(CH$_3$)$_2$), 130.32 (C_{Ar}), 129.40 (C$_{Ar}$CH*C*H), 125.52 (C_{Ar}), 124.68 (*C*HC(CH$_3$)$_2$), 117.12 (C_{Ar}), 116.63 (C_{Ar}), 112.20 (CCH*C*H$_2$), 42.65 (C*C*H$_2$CH$_2$), 41.22 (*C*CH$_2$CH$_2$), 29.72 (C*C*H$_3$), 25.74 (C(*C*H$_3$)$_2$), 23.23 (CCH$_2$*C*H$_2$), 17.70 (C(*C*H$_3$)$_2$). HRMS (ESI) m/z calcd for $C_{20}H_{27}N_3OSNa^+$ (M + Na)$^+$ 380.1767, found 380.1766.

2-((*E*)-5-((*S*,*E*)-3,7-Dimethyl-3-vinylocta-1,6-dien-1-yl)-2-hydroxybenzylidene)-*N*-methylhydrazine-1-carbothioamide (2b). White solid, yield 99%, purity ≥ 95% by HPLC. ^{1}H-NMR (300 MHz, CDCl$_3$) δ 10.02 (s, 1H, CHNN*H*), 9.39 (s, 1H, –O*H*), 8.05 (s, 1H, C*H*NNH), 7.36 (dd, J = 8.6 Hz, 1H, ArH), 7.22 (d, J = 2.1 Hz, 1H, ArH), 6.93 (d, J = 8.5 Hz, 1H, ArH), 6.80–6.71 (m, 1H, N*H*CH$_3$), 6.25 (d, J = 16.3 Hz, 1H, CHC*H*), 6.09 (d, J = 16.3 Hz, 1H, C*H*CH), 5.88 (dd, J = 17.4 Hz, 1H, C*H*C(CH$_3$)$_2$), 5.12 (m, 1H, C*H*CH), 5.06 (dd, J = 7.8 Hz, 1H, CHC*H*$_2$), 5.01 (dd, J = 14.5 Hz, 1H, CHC*H*$_2$), 3.27 (d, J = 4.6 Hz, 3H, NHC*H*$_3$), 1.96 (q, J = 7.6 Hz, 2H, CCH$_2$*CH*$_2$), 1.68 (s, 3H, C(*CH*$_3$)$_2$), 1.58 (s, 3H, C(*CH*$_3$)$_2$), 1.54–1.47 (m, 2H, C*CH*$_2$CH$_2$), 1.20 (s, 3H, C*CH*$_3$). ^{13}C NMR (101 MHz, CDCl$_3$) δ 177.46 (NNH*C*S), 156.24 (C_{Ar}OH), 147.25 (C*C*HCH$_2$), 145.64 (*C*HNNH), 137.02 (C$_{Ar}$*C*HCH), 131.43 (C_{Ar}), 130.55 (*C*C(CH$_3$)$_2$), 129.87 (C_{Ar}), 129.23 (C$_{Ar}$CH*C*H), 125.59 (C_{Ar}), 124.70 (*C*HC(CH$_3$)$_2$), 116.98 (C_{Ar}, C_{Ar}), 112.17 (CCH*C*H$_2$), 42.64 (C*C*H$_2$CH$_2$), 41.23 (*C*CH$_2$CH$_2$), 31.66 (NH*C*H$_3$), 25.74 (C*C*H$_3$), 23.86 (C(*C*H$_3$)$_2$), 23.24 (CCH$_2$*C*H$_2$), 17.69 (C(*C*H$_3$)$_2$). HRMS (ESI) m/z calcd for $C_{21}H_{29}N_3OSNa^+$ (M + Na)$^+$ 394.1923, found 394.1923.

2-((*E*)-5-((*S*,*E*)-3,7-Dimethyl-3-vinylocta-1,6-dien-1-yl)-2-hydroxybenzylidene)-*N*-ethylhydrazine-1-carbothioamide (2c). White solid, yield 96%, purity ≥ 95% by HPLC. ^{1}H-NMR (300 MHz, CDCl$_3$) δ 10.07 (s, 1H, CHNN*H*), 9.41 (s, 1H, –O*H*), 8.06 (s, 1H, C*H*NNH), 7.36 (dd, J = 8.6 Hz, 1H, ArH), 7.22 (d, J = 2.1 Hz, 1H, ArH), 6.93 (d, J = 8.5 Hz, 1H, N*H*CH$_2$CH$_3$), 6.68 (s, 1H, ArH), 6.25 (d, J = 16.3 Hz, 1H, CHC*H*), 6.09 (d, J = 16.3 Hz, 1H, C*H*CH), 5.88 (dd, J = 17.4 Hz, 1H, C*H*C(CH$_3$)$_2$), 5.15–4.98 (m, 3H, CC*H*CH$_2$), 3.76 (m, 2H, NHC*H*$_2$CH$_3$), 2.01–1.91 (m, 2H, CCH$_2$*CH*$_2$), 1.70–1.65 (m, 3H, C(*CH*$_3$)$_2$), 1.58 (s, 3H, C(*CH*$_3$)$_2$), 1.54–1.47 (m, 2H, C*CH*$_2$CH$_2$), 1.31 (t, J = 7.3 Hz, 3H, NHCH$_2$-*CH*$_3$), 1.21 (s, 3H, C*CH*$_3$). ^{13}C NMR (101 MHz, CDCl$_3$) δ 176.29 (NNH*C*S), 156.27 (C_{Ar}OH), 147.25 (C*C*HCH$_2$), 145.65 (*C*HNNH), 136.99 (C$_{Ar}$*C*HCH), 131.43 (C_{Ar}), 130.53 (*C*(CH$_3$)$_2$), 129.85 (C_{Ar}), 129.23 (C$_{Ar}$CH*C*H), 125.61 (C_{Ar}), 124.70 (*C*C(CH$_3$)$_2$), 117.00 (C_{Ar}), 116.95 (C_{Ar}), 112.17 (CCH*C*H$_2$), 42.64 (C*C*H$_2$CH$_2$), 41.24 (*C*CH$_2$CH$_2$), 39.85 (NHCH$_2$CH$_3$), 31.29 (C*C*H$_3$), 25.74 (C(*C*H$_3$)$_2$), 23.24 (CCH$_2$*C*H$_2$), 17.70 (C(*C*H$_3$)$_2$), 14.48 (NHCH$_2$*C*H$_3$). HRMS (ESI) m/z calcd for $C_{22}H_{31}N_3OSNa^+$ (M + Na)$^+$ 408.2080, found 408.2080.

***N*-Benzyl-2-((*E*)-5-((*S*,*E*)-3,7-dimethyl-3-vinylocta-1,6-dien-1-yl)-2-hydroxybenzylidene)hydrazine-1-carbothioamide (2d).** White solid, yield 93%, purity ≥ 95% by HPLC. ^{1}H-NMR (300 MHz, CDCl$_3$) δ 10.16 (s, 1H, CHNN*H*), 9.26 (s, 1H, –O*H*), 8.08 (s, 1H, C*H*NNH), 7.40–7.30 (m, 6H, ArH), 7.19 (d, J = 2.1 Hz, 1H, ArH), 7.00 (t, J = 4.8 Hz, 1H, N*H*CH$_2$Ar), 6.89 (d, J = 8.5 Hz, 1H, ArH), 6.24 (d, J = 16.3 Hz, 1H, CHC*H*), 6.08 (d, J = 16.3 Hz, 1H, C*H*CH), 5.87 (dd, J = 17.4 Hz, 1H, CC*H*CH$_2$), 5.14–5.07 (m, 2H, CC*H*C*H*$_2$), 5.04 (dd, J = 2.8 Hz, 1H, C*H*C(CH$_3$)$_2$), 4.99–4.95 (m, 2H, C*H*$_2$Ar), 1.95 (q, J = 7.6 Hz, 2H, CCH$_2$*CH*$_2$), 1.67 (s, 3H, C(*CH*$_3$)$_2$), 1.58 (s, 3H, C(*CH*$_3$)$_2$), 1.54–1.46 (m, 2H, C*CH*$_2$CH$_2$), 1.20 (s, 3H, C*CH*$_3$). ^{13}C NMR (101 MHz, CDCl$_3$) δ 176.79 (NNH*C*S), 156.26 (C_{Ar}OH), 147.56 (C*C*HCH$_2$), 145.63 (*C*HNNH), 137.03 (C$_{Ar}$*C*HCH), 136.94 (C_{Ar}), 131.43 (C_{Ar}), 130.53 (*C*(CH$_3$)$_2$), 129.96 (C_{Ar}), 129.30 (C$_{Ar}$CH*C*H), 128.95 (C_{Ar}, C_{Ar}), 128.00 (C_{Ar}), 127.67 (C_{Ar}, C_{Ar}), 125.58 (C_{Ar}), 124.69 (*C*HC(CH$_3$)$_2$), 116.98 (C_{Ar}), 116.85 (C_{Ar}), 112.18 (CCH*C*H$_2$), 48.72 (NHC*H*$_2$C$_{Ar}$), 42.64 (C*C*H$_2$CH$_2$), 41.23 (*C*CH$_2$CH$_2$), 29.33 (C*C*H$_3$), 25.74 (C(*C*H$_3$)$_2$), 23.24 (CCH$_2$*C*H$_2$), 17.69 (C(*C*H$_3$)$_2$). HRMS (ESI) m/z calcd for $C_{27}H_{33}N_3OSNa^+$ (M + Na)$^+$ 470.2236, found 470.2239.

2-((*E*)-5-((*S*,*E*)-3,7-Dimethyl-3-vinylocta-1,6-dien-1-yl)-2-hydroxybenzylidene)-*N*-(2-phenoxy-ethyl)hydrazine-1-carbothioamide (2e). Yellow solid, yield 35%, purity ≥ 95% by HPLC ^{1}H-NMR (300 MHz, CDCl$_3$) δ 9.87 (s, 1H, CHNN*H*), 9.34 (s,

1H, –O*H*), 8.02 (s, 1H, C*H*NNH), 7.37 (dd, J = 8.6, 2.1 Hz, 1H, ArH), 7.33–7.27 (m, 2H, ArH), 7.20 (d, J = 2.1 Hz, 1H, ArH), 7.00–6.93 (m, 4H, ArH), 6.25 (d, J = 16.3 Hz, 1H, CHC*H*), 6.09 (d, J = 16.3 Hz, 1H, C*H*CH), 5.88 (dd, J = 17.4 Hz, 1H, C*H*C(CH_3)$_2$), 5.15–5.09 (m, 1H, C*H*CH), 5.07 (dd, J = 7.6 Hz, 1H, CHCH_2), 5.02 (dd, J = 14.3 Hz, 1H, CHCH_2), 4.20 (p, J = 4.5 Hz, 4H, C_2H_4O), 1.96 (q, J = 7.5 Hz, 2H, CCH$_2$CH_2), 1.68 (s, 3H, C(CH_3)$_2$), 1.59 (s, 3H, C(CH_3)$_2$), 1.54–1.47 (m, 2H, CCH_2CH$_2$), 1.21 (s, 3H, CCH_3). ^{13}C NMR (101 MHz, $CDCl_3$) δ 176.67 (NNHCS), 158.24 (C_{Ar}OH), 156.50 (OC_{Ar}), 147.33 (CCHCH$_2$), 145.66 (*C*HNNH), 136.95 (C_{Ar}CHCH), 131.79 (C_{Ar}), 130.43 (*C*C(CH_3)$_2$), 129.94 (C_{Ar}, C_{Ar}), 129.62 (C_{Ar}), 129.26 (C_{Ar}CHCH), 125.62 (C_{Ar}), 124.70 (*C*HC(CH_3)$_2$), 121.40 (C_{Ar}), 117.17 (C_{Ar}), 116.82 (C_{Ar}), 114.58 (C_{Ar}, C_{Ar}), 112.17 (CCH*C*H$_2$), 65.90 (CH$_2$*C*H$_2$O), 44.15 (*C*H$_2$CH$_2$O), 42.65 (CCH_2CH$_2$), 41.24 (*C*CH$_2$CH$_2$), 29.01 (CCH_3), 25.75 (C(*C*H$_3$)$_2$), 23.24 (CCH$_2$*C*H$_2$), 17.70 (C(*C*H$_3$)$_2$). HRMS (ESI) m/z calcd for $C_{28}H_{35}N_3O_2SNa^+$ (M + Na)$^+$ 500.2342, found 500.2344.

2-((*E*)-5-((*S*,*E*)-3,7-Dimethyl-3-vinylocta-1,6-dien-1-yl)-2-hydroxybenzylidene)-*N*-phenylhydrazine-1-carbothioamide (2f). White solid, yield 91%, purity ≥ 95% by HPLC. ^{1}H-NMR (300 MHz, $CDCl_3$) δ 10.36 (s, 1H, CHNN*H*), 9.31 (s, 1H, –O*H*), 8.40 (s, 1H, N*H*Ar), 8.13 (s, 1H, C*H*NNH), 7.57 (d, J = 7.6 Hz, 2H, ArH), 7.47–7.35 (m, 3H, ArH), 7.30 (t, J = 7.4 Hz, 1H, ArH), 7.24 (d, J = 2.0 Hz, 1H, ArH), 6.94 (d, J = 8.5 Hz, 1H, ArH), 6.25 (d, J = 16.3 Hz, 1H, CHC*H*), 6.10 (d, J = 16.3 Hz, 1H, C*H*CH), 5.89 (dd, J = 17.4 Hz, 1H, C*H*C(CH_3)$_2$), 5.16–4.99 (m, 3H, CC*H*CH_2), 1.96 (q, J = 7.4 Hz, 2H, CCH$_2$CH_2), 1.68 (s, 3H, C(CH_3)$_2$), 1.59 (s, 3H, C(CH_3)$_2$), 1.55–1.48 (m, 2H, CCH_2CH$_2$), 1.21 (s, 3H, CCH_3). ^{13}C NMR (101 MHz, $CDCl_3$) δ 175.41 (NNHCS), 156.38 (C_{Ar}OH), 147.97 (CCHCH$_2$), 145.62 (*C*HNNH), 137.30 (C_{Ar}CHCH), 137.09 (C_{Ar}), 131.42 (C_{Ar}), 130.59 (*C*(CH$_3$)$_2$), 130.23 (C_{Ar}), 129.39 (C_{Ar}-CH*C*H), 129.05 (C_{Ar}, C_{Ar}), 126.99 (C_{Ar}, C_{Ar}), 125.55 (C_{Ar}), 125.41 (C_{Ar}), 124.72 (*C*HC(CH$_3$)$_2$), 117.06 (C_{Ar}), 116.88 (C_{Ar}), 112.20 (CCH*C*H$_2$), 42.67 (CCH_2CH$_2$), 41.23 (*C*CH$_2$CH$_2$), 30.82 (CCH_3), 25.76 (C(*C*H$_3$)$_2$), 23.25 (CCH$_2$*C*H$_2$), 17.71 (C(*C*H$_3$)$_2$). HRMS (ESI) m/z calcd for $C_{26}H_{31}N_3OSNa^+$ (M + Na)$^+$ 456.2080, found 456.2081.

2-((*E*)-5-((*S*,*E*)-3,7-Dimethyl-3-vinylocta-1,6-dien-1-yl)-2-hydroxybenzylidene)-*N*-(2-fluorophenyl)hydrazine-1-carbothioamide (2g). White solid, yield 88%, purity ≥ 95% by HPLC. ^{1}H-NMR (300 MHz, $CDCl_3$) δ 10.21 (s, 1H, CHNN*H*), 9.19 (s, 1H, –O*H*), 8.53 (s, 1H, N*H*Ar), 8.37–8.28 (m, 1H, ArH), 8.13 (s, 1H, C*H*NNH), 7.39 (dd, J = 8.6, 2.0 Hz, 1H, ArH), 7.25–7.13 (m, 4H, ArH), 6.96 (d, J = 8.5 Hz, 1H, ArH), 6.26 (d, J = 16.2 Hz, 1H, CHC*H*), 6.10 (d, J = 16.2 Hz, 1H, C*H*CH), 5.89 (dd, J = 17.4 Hz, 1H, C*H*C(CH_3)$_2$), 5.13 (d, J = 7.1 Hz, 1H, C*H*CH), 5.07 (dd, J = 7.6 Hz, 1H, CHCH_2), 5.02 (dd, J = 14.4 Hz, 1H, CHCH_2), 1.96 (q, J = 7.6 Hz, 2H, CCH$_2$CH_2), 1.68 (s, 3H, C(CH_3)$_2$), 1.59 (s, 3H, C(CH_3)$_2$), 1.55–1.48 (m, 2H, CCH_2CH$_2$), 1.21 (s, 3H, CCH_3). ^{13}C NMR (101 MHz, $CDCl_3$) δ 174.97 (NNHCS), 156.47 (C_{Ar}F), 154.07 (C_{Ar}OH), 148.03 (CCHCH$_2$), 145.64 (*C*HNNH), 137.09 (C_{Ar}CHCH), 131.43 (C_{Ar}), 130.60 (*C*C(CH$_3$)$_2$), 130.34 (C_{Ar}), 129.42 (C_{Ar}), 127.41 (C_{Ar}), 125.91 (C_{Ar}), 125.55 (C_{Ar}CHCH), 124.70 (C_{Ar}), 124.19 (*C*HC(CH$_3$)$_2$), 117.21 (C_{Ar}), 116.75 (C_{Ar}), 115.72 (C_{Ar}), 115.52 (C_{Ar}), 112.19 (CCH*C*H$_2$), 42.66 (CCH_2CH$_2$), 41.24 (*C*CH$_2$CH$_2$), 25.75 (CCH_3), 23.98 (C(*C*H$_3$)$_2$), 23.25 (CCH$_2$*C*H$_2$), 17.70 (C(*C*H$_3$)$_2$). HRMS (ESI) m/z calcd for $C_{26}H_{30}FN_3OSNa^+$ (M + Na)$^+$ 474.1985, found 474.1986.

***N*-(4-Chlorophenyl)-2-((*E*)-5-((*S*,*E*)-3,7-dimethyl-3-vinylocta-1,6-dien-1-yl)-2-hydroxybenzylidene)hydrazine-1-carbothioamide (2h).** Yellow solid, yield 73%, purity ≥ 95% by HPLC. ^{1}H-NMR (300 MHz, $CDCl_3$) δ 10.40 (s, 1H, CHNN*H*), 9.23 (s, 1H, –O*H*), 8.35 (s, 1H, N*H*Ar), 8.12 (s, 1H, C*H*NNH), 7.55–7.49 (m, 2H, ArH), 7.42–7.35 (m, 3H, ArH), 7.24 (d, J = 2.1 Hz, 1H, ArH), 6.94 (d, J = 8.5 Hz, 1H, ArH), 6.25 (d, J = 16.3 Hz, 1H, CHC*H*), 6.10 (d, J = 16.3 Hz, 1H, C*H*CH), 5.88 (dd, J = 17.4 Hz, 1H, C*H*C(CH_3)$_2$), 5.15–5.10 (m, 1H, C*H*CH), 5.07 (dd, J = 8.9 Hz, 1H, CHCH_2), 5.05–4.99 (m, 1H, CHCH_2), 1.96 (q, J = 7.6 Hz, 2H, CCH$_2$CH_2), 1.68 (s, 3H, C(CH_3)$_2$), 1.59 (d, J = 1.3 Hz, 3H, C(CH_3)$_2$), 1.55–1.47 (m, 2H, CCH_2CH$_2$), 1.21 (s, 3H, CCH_3). ^{13}C NMR (101 MHz, $CDCl_3$) δ 175.45 (NNHCS), 156.31 (C_{Ar}OH), 147.89 (CCHCH$_2$), 145.58 (*C*HNNH), 137.29 (C_{Ar}), 135.86 (C_{Ar}-*C*HCH), 132.39 (C_{Ar}), 131.45 (C_{Ar}), 130.75 (C_{Ar}), 130.36 (*C*C(CH$_3$)$_2$), 129.36 (C_{Ar}, C_{Ar}), 129.13 (C_{Ar}), 126.54 (C_{Ar}CH*C*H), 125.46 (C_{Ar}, C_{Ar}), 124.67 (*C*HC(CH$_3$)$_2$), 117.13 (C_{Ar}), 116.73 (C_{Ar}), 112.23 (CCH*C*H$_2$), 42.67 (CCH_2CH$_2$), 41.22 (*C*CH$_2$CH$_2$), 31.15 (CCH_3), 25.74 (C(*C*H$_3$)$_2$), 23.24 (CCH$_2$*C*H$_2$), 17.70(C(*C*H$_3$)$_2$). HRMS (ESI) m/z calcd for $C_{26}H_{30}ClN_3OSNa^+$ (M + Na)$^+$ 490.1690, found 490.1692.

2-((*E*)-5-((*S*,*E*)-3,7-Dimethyl-3-vinylocta-1,6-dien-1-yl)-2-hydroxybenzylidene)-*N*-(4-methoxy-phenyl)hydrazine-1-carbothioamide (2i). White solid, yield 95%, purity ≥ 90% by HPLC. ^{1}H-NMR (300 MHz, $CDCl_3$) δ 10.65 (s, 1H, CHNN*H*), 9.38 (s, 1H, –O*H*), 8.28 (s, 1H, N*H*Ar), 8.14 (s, 1H, C*H*NNH), 7.43–7.34 (m, 3H, ArH), 7.24 (d, J = 2.0 Hz, 1H, ArH), 6.94 (dd, J = 8.7 Hz, 3H, ArH), 6.24 (d, J = 16.3 Hz, 1H, CHC*H*), 6.10 (d, J = 16.3 Hz, 1H, C*H*CH), 5.88 (dd, J = 17.4 Hz, 1H, C*H*C(CH$_3$)$_2$), 5.11 (m, 1H, C*H*CH), 5.07 (dd, J = 7.5 Hz, 1H, CHCH_2), 5.02 (dd, J = 14.2 Hz, 1H, CHCH_2), 3.83 (s, 3H, OCH_3), 1.96 (q, J = 7.5 Hz, 2H, CCH$_2$CH_2), 1.68 (s, 3H, C(CH_3)$_2$), 1.59 (s, 3H, C(CH_3)$_2$), 1.55–1.46 (m, 2H, CCH_2CH$_2$), 1.21 (s, 3H, CCH_3). ^{13}C NMR (101 MHz, $CDCl_3$) δ 176.08 (NNHCS), 158.53 (C_{Ar}OH), 156.38 (C_{Ar}OCH$_3$), 147.86 (CCHCH$_2$), 145.62 (*C*HNNH), 137.07 (C_{Ar}CHCH), 131.40 (C_{Ar}), 131.18 (*C*C(CH$_3$)$_2$), 130.55 (C_{Ar}), 130.17 (C_{Ar}), 130.03 (C_{Ar}), 129.35 (C_{Ar}CH*C*H), 127.54 (C_{Ar}), 125.54 (C_{Ar}), 124.72 (*C*HC(CH$_3$)$_2$), 117.04 (C_{Ar}), 116.90 (C_{Ar}), 114.26 (C_{Ar}, C_{Ar}), 112.19 (CCH*C*H$_2$), 55.48 (C_{Ar}O*C*H$_3$), 42.66 (CCH_2CH$_2$), 41.23 (*C*CH$_2$CH$_2$), 28.05 (CCH_3), 25.75 (C(*C*H$_3$)$_2$), 23.25 (CCH$_2$*C*H$_2$), 17.71 (C(*C*H$_3$)$_2$). HRMS (ESI) m/z calcd for $C_{27}H_{33}N_3O_2SNa^+$ (M + Na)$^+$ 486.2185, found 486.2187.

2-((*E*)-5-((*S*,*E*)-3,7-Dimethyl-3-vinylocta-1,6-dien-1-yl)-2-hydroxybenzylidene)-*N*-(4-ethoxy-phenyl)hydrazine-1-carbothioamide (2j). White solid, yield 63%, purity ≥ 95% by HPLC. ^{1}H-NMR (300 MHz, $CDCl_3$) δ 10.38 (s, 1H, CHNN*H*), 9.38 (s, 1H, –O*H*), 8.25 (s, 1H, N*H*Ar), 8.11 (s, 1H, C*H*NNH), 7.38 (t, J = 9.0 Hz, 3H, ArH), 7.23 (d, J = 2.0 Hz, 1H, ArH), 6.93 (d, J = 8.8 Hz, 3H, ArH), 6.25 (d, J = 16.3 Hz, 1H, CHC*H*), 6.10 (d, J = 16.3 Hz, 1H, C*H*CH), 5.88 (dd, J = 17.4 Hz, 1H, C*H*C(CH$_3$)$_2$), 5.15–5.09 (m, 1H, C*H*CH), 5.07 (dd, J = 7.5 Hz, 1H, CHCH_2), 5.02 (dd, J = 14.2 Hz, 1H, CHCH_2), 4.05 (q, J = 7.0 Hz, 2H, OCH_2CH$_3$), 1.96 (q, J = 7.5 Hz, 2H, CCH$_2$CH_2), 1.68 (s, 3H, C(CH_3)$_2$), 1.59 (s, 3H, C(CH_3)$_2$), 1.55–1.47 (m, 2H, CCH_2CH$_2$), 1.43 (t, J = 7.0 Hz, 3H, OCH$_2$CH_3), 1.21 (s, 3H, CCH_3). ^{13}C NMR (101 MHz, $CDCl_3$) δ 176.09 (NNHCS), 157.94 (C_{Ar}OH), 156.39 (C_{Ar}OC$_2$H$_5$), 147.71

(C*C*HCH$_2$), 145.63 (*C*HNNH), 137.07 (C$_{Ar}$*C*HCH), 131.40 (*C*$_{Ar}$), 130.55 (*C*(CH$_3$)$_2$), 130.15 (*C*$_{Ar}$), 129.86 (*C*$_{Ar}$), 129.32 (C$_{Ar}$CH*C*H), 127.42 (*C*$_{Ar}$, *C*$_{Ar}$), 125.55 (*C*$_{Ar}$), 124.72 (*C*HC(CH$_3$)$_2$), 117.05 (*C*$_{Ar}$, *C*$_{Ar}$), 116.90 (*C*$_{Ar}$), 114.75 (*C*$_{Ar}$), 112.18 (CCH*C*H$_2$), 63.70 (NH*C*H$_2$CH$_3$), 42.65 (C*C*H$_2$CH$_2$), 41.23 (*C*CH$_2$CH$_2$), 25.73 (C*C*H$_3$), 23.84 (C(*C*H$_3$)$_2$), 23.24 (CCH$_2$*C*H$_2$), 17.70 (C(*C*H$_3$)$_2$), 14.84 (NHCH$_2$*C*H$_3$). HRMS (ESI) *m*/*z* calcd for C$_{28}$H$_{35}$N$_3$O$_2$SNa$^+$ (M + Na)$^+$ 500.2342, found 500.2342.

2-((*E*)-5-((*S*,*E*)-3,7-Dimethyl-3-vinylocta-1,6-dien-1-yl)-2-hydroxybenzylidene)-*N*-(4-(trifluoro-methyl)phenyl)hydrazine-1-carbothioamide (2k). White solid, yield 99%, purity ≥ 90% by HPLC. ^{1}H-NMR (300 MHz, CDCl$_3$) *δ* 10.21 (s, 1H, CHNN*H*), 9.15 (s, 1H, –O*H*), 8.51 (s, 1H, N*H*Ar), 8.12 (s, 1H, C*H*NNH), 7.79 (d, *J* = 8.5 Hz, 2H, ArH), 7.67 (d, *J* = 8.6 Hz, 2H, ArH), 7.40 (dd, *J* = 8.6 Hz, 1H, ArH), 7.25 (d, *J* = 2.1 Hz, 1H, ArH), 6.95 (d, *J* = 8.5 Hz, 1H, ArH), 6.26 (d, *J* = 16.3 Hz, 1H, CHC*H*), 6.11 (d, *J* = 16.3 Hz, 1H, C*H*CH), 5.88 (dd, *J* = 17.4 Hz, 1H, C*H*C(CH$_3$)$_2$), 5.12 (m, 1H, C*H*CH), 5.09–5.05 (m, 1H, CHC*H*$_2$), 5.02 (dd, *J* = 15.5 Hz, 1H, CHC*H*$_2$), 2.01–1.91 (m, 2H, CCH$_2$*C*H$_2$), 1.68 (s, 3H, C(*C*H$_3$)$_2$), 1.59 (s, 3H, C(*C*H$_3$)$_2$), 1.55–1.48 (m, 2H, C*C*H$_2$CH$_2$), 1.21 (s, 3H, C*C*H$_3$). ^{13}C NMR (101 MHz, CDCl$_3$) *δ* 175.03 (NNH*C*S), 156.30 (*C*$_{Ar}$OH), 147.92 (C*C*HCH$_2$), 145.56 (*C*HNNH), 140.48 (*C*$_{Ar}$), 137.39 (C$_{Ar}$*C*HCH), 131.47 (*C*$_{Ar}$), 130.84 (*C*$_{Ar}$), 130.48 (*C*C(CH$_3$)$_2$), 129.35 (*C*$_{Ar}$), 128.18 (C$_{Ar}$CH*C*H), 126.17 (*C*$_{Ar}$, *C*$_{Ar}$, *C*$_{Ar}$), 125.42 (*C*$_{Ar}$, *C*$_{Ar}$), 124.65 (*C*HC(CH$_3$)$_2$), 124.38 (C$_{Ar}$*C*F$_3$), 117.19 (*C*$_{Ar}$), 116.67 (*C*$_{Ar}$), 112.24 (CCH*C*H$_2$), 42.67 (C*C*H$_2$CH$_2$), 41.22 (*C*CH$_2$CH$_2$), 25.72 (C*C*H$_3$), 23.91 (C(*C*H$_3$)$_2$), 23.23 (CCH$_2$*C*H$_2$), 17.68 (C(*C*H$_3$)$_2$). HRMS (ESI) *m*/*z* calcd for C$_{27}$H$_{30}$F$_3$N$_3$OSNa$^+$ (M + Na)$^+$ 524.1953, found 524.1956.

***N*-(3,5-Bis(trifluoromethyl)phenyl)-2-((*E*)-5-((*S*,*E*)-3,7-dimethyl-3-vinylocta-1,6-dien-1-yl)-2-hydroxybenzylidene) hydrazine-1-carbothioamide (2l).** Yellow solid, yield 99%, purity ≥ 90% by HPLC. ^{1}H-NMR (400 MHz, CDCl$_3$) *δ* 10.19 (s, 1H, CHNN*H*), 9.02 (s, 1H, –O*H*), 8.61 (d, *J* = 8.5 Hz, 1H, C*H*NNH), 8.21–8.11 (m, 3H, ArH), 7.76 (s, 1H, ArH), 7.44–7.36 (m, 1H, ArH), 6.98 (dd, *J* = 25.9 Hz, 1H, ArH), 6.27 (dd, *J* = 16.2 Hz, 1H, CHC*H*), 6.12 (dd, *J* = 16.2 Hz, 1H, C*H*CH), 5.89 (m, 1H, C*H*C(CH$_3$)$_2$), 5.15–5.09 (m, 1H, C*H*CH), 5.08–5.05 (m, 1H, CHC*H*$_2$), 5.05–5.00 (m, 1H, CHC*H*$_2$), 1.95 (q, *J* = 7.3 Hz, 2H, CCH$_2$*C*H$_2$), 1.68 (s, 3H, C(*C*H$_3$)$_2$), 1.59 (d, *J* = 3.7 Hz, 3H, C(*C*H$_3$)$_2$), 1.54–1.48 (m, 2H, C*C*H$_2$CH$_2$), 1.22 (d, *J* = 4.7 Hz, 3H, C*C*H$_3$). ^{13}C NMR (101 MHz, CDCl$_3$) *δ* 175.22 (NNH*C*S), 156.24 (*C*$_{Ar}$OH), 148.40 (C*C*HCH$_2$), 145.70 (*C*HNNH), 145.52 (*C*$_{Ar}$), 138.91 (C$_{Ar}$*C*HCH), 137.49 (*C*$_{Ar}$), 132.37 (*C*$_{Ar}$), 132.04 (*C*$_{Ar}$), 131.47 (*C*$_{Ar}$), 131.44 (*C*$_{Ar}$), 130.96 (*C*(CH$_3$)$_2$), 130.67 (*C*$_{Ar}$), 129.36 (C$_{Ar}$CH*C*H), 125.36 (*C*$_{Ar}$), 124.72 (*C*HC(CH$_3$)$_2$), 124.64 (*C*F$_3$), 124.29 (*C*F$_3$), 121.58 (*C*$_{Ar}$), 117.21 (*C*$_{Ar}$), 116.57 (*C*$_{Ar}$), 112.25 (CCH*C*H$_2$), 42.67 (C*C*H$_2$CH$_2$), 41.19 (*C*CH$_2$CH$_2$), 25.72 (C*C*H$_3$), 23.22 (C(*C*H$_3$)$_2$), 23.18 (CCH$_2$*C*H$_2$), 17.67 (C(*C*H$_3$)$_2$). HRMS (ESI) *m*/*z* calcd for C$_{28}$H$_{29}$F$_6$N$_3$OSNa$^+$ (M + Na)$^+$ 592.1827, found 592.1829.

***N*-Cyclohexyl-2-((*E*)-5-((*S*,*E*)-3,7-dimethyl-3-vinylocta-1,6-dien-1-yl)-2-hydroxybenzylidene)hydrazine-1-carbothioamide (2m).** White solid, yield 61%, purity ≥ 95% by HPLC. ^{1}H-NMR (300 MHz, CDCl$_3$) *δ* 10.05 (s, 1H, CHNN*H*), 9.47 (s, 1H, –O*H*), 8.06 (s, 1H, C*H*NNH), 7.36 (dd, *J* = 8.6 Hz, 1H, ArH), 7.22 (d, *J* = 2.1 Hz, 1H, ArH), 6.93 (d, *J* = 8.5 Hz, 1H, ArH), 6.58 (d, *J* = 7.8 Hz, 1H, N*H*C$_6$H$_{11}$), 6.25 (d, *J* = 16.3 Hz, 1H, CHC*H*), 6.09 (d, *J* = 16.3 Hz, 1H, C*H*CH), 5.88 (dd, *J* = 17.4 Hz, 1H, C*H*C(CH$_3$)$_2$), 5.15–4.98 (m, 3H, C*CH*CH$_2$), 4.29 (m, 1H, NHC*H*C$_5$H$_{10}$), 2.11 (dd, *J* = 12.0 Hz, 2H, C$_5$H$_{10}$), 2.01–1.91 (m, 2H, CCH$_2$*C*H$_2$), 1.80–1.70 (m, 2H, C$_5$H$_{10}$), 1.69–1.66 (m, 3H, C(*C*H$_3$)$_2$), 1.58 (s, 3H, C(*C*H$_3$)$_2$), 1.51 (dd, *J* = 7.2, 4.1 Hz, 2H, C*C*H$_2$CH$_2$), 1.49–1.25 (m, 6H, C$_5$H$_{10}$), 1.21 (s, 3H, C*C*H$_3$). ^{13}C NMR (101 MHz, CDCl$_3$) *δ* 175.06 (NNH*C*S), 156.33 (*C*$_{Ar}$OH), 147.00 (C*C*HCH$_2$), 145.65 (*C*HNNH), 136.97 (C$_{Ar}$*C*HCH), 131.43 (*C*$_{Ar}$), 130.49 (*C*(CH$_3$)$_2$), 129.86 (*C*$_{Ar}$), 129.18 (C$_{Ar}$CH*C*H), 125.62 (*C*$_{Ar}$), 124.70 (*C*C(CH$_3$)$_2$), 117.03 (*C*$_{Ar}$), 116.93 (*C*$_{Ar}$), 112.17 (CCH*C*H$_2$), 53.34 (NH*C*HC$_5$H$_{10}$), 42.64 (C*C*H$_2$CH$_2$), 41.24 (*C*CH$_2$CH$_2$), 32.64 (NHCH*C*$_5$H$_{10}$), 27.19 (C*C*H$_3$), 25.74 (C(*C*H$_3$)$_2$), 25.41 (NHCH*C*$_5$H$_{10}$), 24.66 (NHCH*C*$_5$H$_{10}$), 23.25 (NHCH*C*$_5$H$_{10}$, NHCH*C*$_5$H$_{10}$), 23.24 (CCH$_2$*C*H$_2$), 17.70 (C(*C*H$_3$)$_2$). HRMS (ESI) *m*/*z* calcd for C$_{26}$H$_{37}$N$_3$OSNa$^+$ (M + Na)$^+$ 462.2549, found 462.2550.

2-((*E*)-5-((*S*,*E*)-3,7-Dimethyl-3-vinylocta-1,6-dien-1-yl)-2-hydroxybenzylidene)-*N*-(piperidin-1-yl)hydrazine-1-carbothioamide (2n). Yellow solid, yield 32%, purity ≥ 95% by HPLC. ^{1}H-NMR (300 MHz, CDCl$_3$) *δ* 11.21 (s, 1H, CHNN*H*), 10.23 (s, 1H, –O*H*), 8.15 (s, 1H, C*H*NNH), 7.49 (s, 1H, NN*H*), 7.34 (dd, *J* = 8.6 Hz, 1H, ArH), 7.16 (d, *J* = 2.1 Hz, 1H, ArH), 6.98 (d, *J* = 8.5 Hz, 1H, ArH), 6.24 (d, *J* = 16.2 Hz, 1H, CHC*H*), 6.05 (d, *J* = 16.2 Hz, 1H, C*H*CH), 5.88 (dd, *J* = 17.4 Hz, 1H, C*H*C(CH$_3$)$_2$), 5.14–5.07 (m, 1H, C*H*CH), 5.07–5.04 (m, 1H, CHC*H*$_2$), 5.01 (dd, *J* = 12.5 Hz, 1H, CHC*H*$_2$), 3.14 (d, *J* = 9.1 Hz, 2H, C$_5$H$_{10}$), 2.57–2.39 (m, 2H, C$_5$H$_{10}$), 1.95 (q, *J* = 7.5 Hz, 2H, CCH$_2$*C*H$_2$), 1.87–1.60 (m, 9H, C$_5$H$_{10}$, C(*C*H$_3$)$_2$), 1.58 (s, 3H, C(*C*H$_3$)$_2$), 1.53–1.46 (m, 2H, C*C*H$_2$CH$_2$), 1.20 (s, 3H, C*C*H$_3$). ^{13}C NMR (101 MHz, CDCl$_3$) *δ* 177.16 (NNH*C*S), 157.52 (*C*$_{Ar}$OH), 148.12 (C*C*HCH$_2$), 145.84 (*C*HNNH), 136.10 (C$_{Ar}$*C*HCH), 131.40 (*C*$_{Ar}$), 129.38 (*C*C(CH$_3$)$_2$), 129.30 (*C*$_{Ar}$), 127.98 (C$_{Ar}$CH*C*H), 125.97 (*C*$_{Ar}$), 124.73 (*C*HC(CH$_3$)$_2$), 117.73 (*C*$_{Ar}$), 117.26 (*C*$_{Ar}$), 112.02 (CCH*C*H$_2$), 56.89 (NC$_5$H$_{10}$, NC$_5$H$_{10}$), 42.56 (C*C*H$_2$CH$_2$), 41.29 (*C*CH$_2$CH$_2$), 25.73 (C*C*H$_3$), 25.57 (NC$_5$H$_{10}$, NC$_5$H$_{10}$), 23.33 (C(*C*H$_3$)$_2$), 23.24 (CCH$_2$*C*H$_2$), 22.78 (NC$_5$H$_{10}$), 17.69 (C(*C*H$_3$)$_2$). HRMS (ESI) *m*/*z* calcd for C$_{25}$H$_{36}$N$_4$OSNa$^+$ (M + Na)$^+$ 463.2502, found 463.2502.

2-((*E*)-5-((*S*,*E*)-3,7-Dimethyl-3-vinylocta-1,6-dien-1-yl)-2-hydroxybenzylidene)-*N*-morpholinohy-drazine-1-carbothioamide (2o). Yellow solid, yield 59%, purity ≥ 95% by HPLC. ^{1}H-NMR (300 MHz, CDCl$_3$) *δ* 11.14 (s, 1H, CHNN*H*), 10.22 (s, 1H, –O*H*), 8.19 (s, 1H, C*H*NNH), 7.56 (s, 1H, NN*H*), 7.35 (dd, *J* = 8.6 Hz, 1H, ArH), 7.16 (d, *J* = 1.9 Hz, 1H, ArH), 6.98 (d, *J* = 8.6 Hz, 1H, ArH), 6.23 (d, *J* = 16.2 Hz, 1H, CHC*H*), 6.05 (d, *J* = 16.2 Hz, 1H, C*H*CH), 5.88 (dd, *J* = 17.4 Hz, 1H, C*H*C(CH$_3$)$_2$), 5.10 (m, 1H, C*H*CH), 5.05 (dd, *J* = 6.6 Hz, 1H, CHC*H*$_2$), 5.01 (dd, *J* = 13.3 Hz, 1H, CHC*H*$_2$), 3.83 (dd, *J* = 69.3 Hz, 4H, C$_2$H$_4$OC$_2$H$_4$S), 2.92 (dd, *J* = 68.1 Hz, 4H, C$_2$H$_4$OC$_2$H$_4$S), 1.95 (q, *J* = 7.5 Hz, 2H, CCH$_2$*C*H$_2$), 1.67 (s, 3H, C(*C*H$_3$)$_2$), 1.58 (s, 3H, C(*C*H$_3$)$_2$), 1.53–1.46 (m, 2H, C*C*H$_2$CH$_2$), 1.20 (s, 3H, C*C*H$_3$). ^{13}C NMR (101 MHz, CDCl$_3$) *δ* 177.18 (NNH*C*S), 157.47 (*C*$_{Ar}$OH), 148.66 (C*C*HCH$_2$), 145.79 (*C*HNNH), 136.26 (C$_{Ar}$*C*HCH), 131.42 (*C*$_{Ar}$), 129.55 (*C*C(CH$_3$)$_2$), 129.42 (*C*$_{Ar}$), 128.11 (C$_{Ar}$CH*C*H), 125.88 (*C*$_{Ar}$), 124.71 (*C*HC(CH$_3$)$_2$), 117.74 (*C*$_{Ar}$), 117.13 (*C*$_{Ar}$), 112.06 (CCH*C*H$_2$), 66.38 (NC$_4$H$_8$O, NC$_4$H$_8$O), 55.90 (NC$_4$H$_8$O, NC$_4$H$_8$O), 42.57 (C*C*H$_2$CH$_2$), 41.28 (*C*CH$_2$CH$_2$), 25.73 (C*C*H$_3$), 23.31 (C(*C*H$_3$)$_2$), 23.24 (CCH$_2$*C*H$_2$), 17.69 (C(*C*H$_3$)$_2$). HRMS (ESI) *m*/*z* calcd for C$_{24}$H$_{34}$N$_4$O$_2$SNa$^+$ (M + Na)$^+$ 465.2294, found 465.2296.

2-((*E*)-5-((*S*,*E*)-3,7-Dimethyl-3-vinylocta-1,6-dien-1-yl)-2-hydroxybenzylidene)-*N*-(pyridin-3-yl)hydrazine-1-carbothioamide (2p). Yellow solid, yield 78%, purity ≥ 95% by HPLC. ^{1}H-NMR (300 MHz, $CDCl_3$) δ 10.44 (s, 1H, CHNN*H*), 8.76 (d, J = 2.4 Hz, 1H, C*H*NNH), 8.61 (s, 1H, –O*H*), 8.50 (dd, J = 4.8, 1.3 Hz, 1H, ArH), 8.15 (d, J = 6.3 Hz, 2H, ArH), 7.41–7.34 (m, 2H, ArH), 7.27 (s, 1H, ArH), 6.93 (d, J = 8.5 Hz, 1H, ArH), 6.24 (d, J = 16.3 Hz, 1H, CHC*H*), 6.09 (d, J = 16.3 Hz, 1H, C*H*CH), 5.88 (dd, J = 17.4 Hz, 1H, C*H*C(CH_3)$_2$), 5.14–5.08 (m, 1H, C*H*CH), 5.06 (dd, J = 8.1 Hz, 1H, CHCH_2), 5.01 (dd, J = 14.8 Hz, 1H, CHCH_2), 2.00–1.90 (m, 2H, CCH$_2$CH_2), 1.67 (s, 3H, C(CH_3)$_2$), 1.58 (s, 3H, C(CH_3)$_2$), 1.54–1.46 (m, 2H, CCH_2CH$_2$), 1.20 (s, 3H, CCH_3). ^{13}C NMR (101 MHz, $CDCl_3$) δ 175.87 (NNHCS), 156.35 (C_{Ar}OH), 147.60 (C*C*HCH$_2$), 147.25 (*C*HNNH), 146.12 (C_{Ar}), 145.60 (C_{Ar}), 137.19 (C_{Ar}*C*HCH), 134.62 (C_{Ar}), 132.90 (C_{Ar}), 131.43 (*C*C(CH$_3$)$_2$), 130.67 (C_{Ar}), 130.28 (C_{Ar}), 128.94 (C_{Ar}CH*C*H), 125.53 (C_{Ar}), 124.68 (*C*HC(CH$_3$)$_2$), 123.45 (C_{Ar}), 117.16 (C_{Ar}), 117.00 (C_{Ar}), 112.20 (CCH*C*H$_2$), 42.66 (C*C*H$_2$CH$_2$), 41.22 (*C*CH$_2$CH$_2$), 25.74 (C*C*H$_3$), 24.14 (C(*C*H$_3$)$_2$), 23.23 (CCH$_2$*C*H$_2$), 17.70 (C(*C*H$_3$)$_2$). HRMS (ESI) m/z calcd for $C_{25}H_{30}N_4OSNa^+$ (M + Na)$^+$ 457.2032, found 457.2030.

2-((*E*)-5-((*S*,*E*)-3,7-Dimethyl-3-vinylocta-1,6-dien-1-yl)-2-hydroxybenzylidene)-*N*-(furan-2-ylmethyl)hydrazine-1-carbothioamide (2q). Yellow solid, yield 43%, purity ≥ 95% by HPLC. ^{1}H-NMR (300 MHz, $CDCl_3$) δ 10.14 (s, 1H, CHNN*H*), 9.31 (s, 1H, –O*H*), 8.07 (s, 1H, C*H*NNH), 7.40–7.33 (m, 2H, ArH), 7.21 (d, J = 2.1 Hz, 1H, ArH), 6.98 (t, J = 5.3 Hz, 1H, N*H*CH$_2$), 6.92 (d, J = 8.5 Hz, 1H, C$_4$*H*$_3$O), 6.38–6.33 (m, 2H, C$_4$*H*$_3$O), 6.25 (d, J = 16.3 Hz, 1H, CHC*H*), 6.09 (d, J = 16.3 Hz, 1H, C*H*CH), 5.88 (dd, J = 17.4 Hz, 1H, C*H*C(CH$_3$)$_2$), 5.15–5.09 (m, 1H, C*H*CH), 5.06 (dd, J = 7.7 Hz, 1H, CHCH_2), 5.01 (dd, J = 14.4 Hz, 1H, CHCH_2), 4.95 (d, J = 5.4 Hz, 2H, NHCH_2), 1.95 (q, J = 7.5 Hz, 2H, CCH$_2$CH_2), 1.67 (s, 3H, C(CH_3)$_2$), 1.58 (s, 3H, C(CH_3)$_2$), 1.54–1.47 (m, 2H, CCH_2CH$_2$), 1.20 (s, 3H, CCH_3). ^{13}C NMR (101 MHz, $CDCl_3$) δ 176.58 (NNHCS), 156.30 (C_{Ar}OH), 149.80 (C*C*HCH$_2$), 147.48 (*C*HNNH), 145.63 (C_{Ar}), 142.71 (C_{Ar}), 137.05 (C_{Ar}*C*HCH), 131.44 (C_{Ar}), 130.54 (*C*C(CH$_3$)$_2$), 130.03 (C_{Ar}), 129.27 (C_{Ar}CH*C*H), 125.57 (C_{Ar}), 124.68 (*C*HC(CH$_3$)$_2$), 117.03 (C_{Ar}), 116.81 (C_{Ar}), 112.18 (C_{Ar}), 110.59 (C_{Ar}), 108.47 (CCH*C*H$_2$), 42.64 (NH*C*H$_2$), 41.75 (C*C*H$_2$CH$_2$), 41.23 (*C*CH$_2$CH$_2$), 25.73 (C*C*H$_3$), 23.50 (C(*C*H$_3$)$_2$), 23.25 (CCH$_2$*C*H$_2$), 17.69(C(*C*H$_3$)$_2$). HRMS (ESI) m/z calcd for $C_{25}H_{31}N_3O_2SNa^+$ (M + Na)$^+$ 460.2029, found 460.2029.

2-((*E*)-5-((*S*,*E*)-3,7-Dimethyl-3-vinylocta-1,6-dien-1-yl)-2-hydroxybenzylidene)-*N*-(thiophen-2-ylmethyl)hydrazine-1-carbothioamide (2r). Yellow solid, yield 29%, purity ≥ 90% by HPLC. ^{1}H-NMR (300 MHz, $CDCl_3$) δ 10.26 (s, 1H, CHNN*H*), 9.31 (s, 1H, –O*H*), 8.11 (s, 1H, C*H*NNH), 7.36 (dd, J = 8.6 Hz, 1H, C$_4$*H*$_3$S), 7.24 (dd, J = 5.1 Hz, 1H, C$_4$*H*$_3$S), 7.21 (d, J = 2.1 Hz, 1H, C$_4$*H*$_3$S), 7.10–7.07 (m, 1H, ArH), 7.03–6.94 (m, 2H, ArH), 6.90 (d, J = 8.5 Hz, 1H, N*H*CH$_2$), 6.24 (d, J = 16.3 Hz, 1H, CHC*H*), 6.08 (d, J = 16.3 Hz, 1H, C*H*CH), 5.87 (dd, J = 17.4 Hz, 1H, C*H*C(CH$_3$)$_2$), 5.13 (d, J = 5.4 Hz, 2H, NHCH_2), 5.11–5.08 (m, 1H, C*H*CH$_2$), 5.06 (dd, J = 7.7 = Hz, 1H, CHCH_2), 5.01 (dd, J = 14.4 Hz, 1H, CHCH_2), 1.95 (q, J = 7.3 Hz, 2H, CCH$_2$CH_2), 1.67 (s, 3H, C(CH_3)$_2$), 1.58 (s, 3H, C(CH_3)$_2$), 1.54–1.46 (m, 2H, CCH_2CH$_2$), 1.20 (s, 3H, CCH_3). ^{13}C NMR (101 MHz, $CDCl_3$) δ 176.46 (NNHCS), 156.27 (C_{Ar}OH), 147.51 (C*C*HCH$_2$), 145.62 (*C*HNNH), 139.29 (NHCH$_2$*C*S), 137.07 (C_{Ar}*C*HCH), 131.44 (C_{Ar}), 130.55 (*C*C(CH$_3$)$_2$), 130.05 (C_{Ar}), 129.26 (C_{Ar}CH*C*H), 126.98 (C_{Ar}), 126.77 (C_{Ar}), 125.87 (C_{Ar}), 125.56 (C_{Ar}), 124.68 (*C*HC(CH$_3$)$_2$), 117.03 (C_{Ar}), 116.79 (C_{Ar}), 112.19 (CCH*C*H$_2$), 43.56 (CNH*C*H$_2$), 42.64 (C*C*H$_2$CH$_2$), 41.23 (*C*CH$_2$CH$_2$), 29.72 (C*C*H$_3$), 25.74 (C(*C*H$_3$)$_2$), 23.23 (CCH$_2$*C*H$_2$), 17.69 (C(*C*H$_3$)$_2$). HRMS (ESI) m/z calcd for $C_{25}H_{31}N_3OS_2Na^+$ (M + Na)$^+$ 476.1800, found 476.1803.

***N*-(Benzo[*d*]thiazol-2-yl)-2-((*E*)-5-((*S*,*E*)-3,7-dimethyl-3-vinylocta-1,6-dien-1-yl)-2-hydroxybenzylidene)hydrazine-1-carbothioamide (2s).** Yellow solid, yield 45%, purity ≥ 95% by HPLC. ^{1}H-NMR (300 MHz, $CDCl_3$) δ 10.59 (s, 1H, N*H*CN), 8.28 (s, 1H, C*H*NNH), 7.54 (d, J = 7.8 Hz, 1H, ArH), 7.38–7.28 (m, 3H, ArH), 7.18–7.08 (m, 2H, ArH), 6.98 (d, J = 8.5 Hz, 1H, ArH), 6.22 (d, J = 16.2 Hz, 1H, CHC*H*), 6.04 (d, J = 16.2 Hz, 1H, C*H*CH), 5.87 (dd, J = 17.4 Hz, 1H, C*H*C(CH$_3$)$_2$), 5.14–5.07 (m, 1H, C*H*CH$_2$), 5.05 (dd, J = 7.0 Hz, 1H, CHCH_2), 5.00 (dd, J = 13.7 Hz, 1H, CHCH_2), 2.00–1.88 (m, 2H, CCH$_2$CH_2), 1.67 (s, 3H, C(CH_3)$_2$), 1.58 (s, 3H, C(CH_3)$_2$), 1.53–1.44 (m, 2H, CCH_2CH$_2$), 1.19 (s, 3H, CCH_3). ^{13}C NMR (101 MHz, $CDCl_3$) δ 168.05 (NNHCS), 160.38 (NHCNHCS), 157.14 (C_{Ar}OH), 150.53 (NHCNCCS), 145.78 (C*C*HCH$_2$), 144.69 (*C*HNNH), 136.16 (C_{Ar}*C*HCH), 131.36 (C_{Ar}), 129.56 (*C*C(CH$_3$)$_2$), 129.04 (NHCNC*C*S), 128.38 (C_{Ar}, C_{Ar}), 126.58 (C_{Ar}CH*C*H), 125.92 (C_{Ar}), 124.74 (*C*HC(CH$_3$)$_2$), 122.51 (C_{Ar}), 122.03 (C_{Ar}), 117.62 (C_{Ar}), 116.89 (C_{Ar}), 114.55 (C_{Ar}), 112.03 (CCH*C*H$_2$), 42.57 (C*C*H$_2$CH$_2$), 41.24 (*C*CH$_2$CH$_2$), 28.39 (C*C*H$_3$), 25.73 (C(*C*H$_3$)$_2$), 23.24 (CCH$_2$*C*H$_2$), 17.67 (C(*C*H$_3$)$_2$). HRMS (ESI) m/z calcd for $C_{27}H_{31}N_4OS_2^+$ (M + H)$^+$ 491.1933, found 491.1933.

***N*-(2-(1*H*-Indol-3-yl)ethyl)-2-((*E*)-5-((*S*,*E*)-3,7-dimethyl-3-vinylocta-1,6-dien-1-yl)-2-hydroxybenzylidene)hydrazine-1-carbothioamide (2t).** Yellow solid, yield 28%, purity ≥ 95% by HPLC. ^{1}H-NMR (300 MHz, $CDCl_3$) δ 9.83 (s, 1H, CHNN*H*), 9.07 (s, 1H, –O*H*), 8.17 (d, J = 9.3 Hz, 1H, CHN*H*), 7.94 (s, 1H, C*H*NNH), 7.66 (d, J = 7.8 Hz, 1H, N*H*C$_2$H$_4$), 7.45–7.31 (m, 2H, ArH), 7.24–7.07 (m, 4H, ArH), 6.91 (d, J = 8.5 Hz, 1H, ArH), 6.79 (t, J = 5.2 Hz, 1H, ArH), 6.29–6.20 (m, 1H, CHC*H*), 6.14–6.05 (m, 1H, C*H*CH), 5.89 (m, 1H, C*H*C(CH$_3$)$_2$), 5.15–5.09 (m, 1H, C*H*CH), 5.07 (dd, J = 8.0 Hz, 1H, CHCH_2), 5.02 (dd, J = 14.6 Hz, 1H, CHCH_2), 4.02 (q, J = 6.3 Hz, 2H, NHC$_2$*H*$_4$), 3.16 (t, J = 6.5 Hz, 2H, NHC$_2$*H*$_4$), 1.96 (q, J = 7.5 Hz, 2H, CCH$_2$CH_2), 1.68 (s, 3H, C(CH_3)$_2$), 1.59 (s, 3H, C(CH_3)$_2$), 1.51 (dd, J = 10.2, 6.8 Hz, 2H, CCH_2CH$_2$), 1.21 (s, 3H, CCH_3). ^{13}C NMR (101 MHz, $CDCl_3$) δ 176.27 (NNHCS), 156.21 (C_{Ar}OH), 146.63 (C*C*HCH$_2$), 145.65 (*C*HNNH), 137.00 (C_{Ar}), 136.75 (C_{Ar}*C*HCH), 132.93 (C_{Ar}), 131.45 (*C*C(CH$_3$)$_2$), 130.47 (C_{Ar}), 129.77 (C_{Ar}CH*C*H), 129.23 (C_{Ar}), 126.83 (C_{Ar}), 125.58 (C_{Ar}), 124.69 (*C*HC(CH$_3$)$_2$), 122.54 (C_{Ar}), 122.39 (C_{Ar}), 119.68 (C_{Ar}), 118.82 (C_{Ar}), 116.97 (C_{Ar}), 112.35 (C_{Ar}), 112.17 (C_{Ar}), 111.44 (CCH*C*H$_2$), 44.58 (NH*C*H$_2$CH$_2$), 42.64 (C*C*H$_2$CH$_2$), 41.23 (*C*CH$_2$CH$_2$), 30.20 (NHCH$_2$*C*H$_2$), 25.74 (C*C*H$_3$), 24.76 (C(*C*H$_3$)$_2$), 23.25 (CCH$_2$*C*H$_2$), 17.69 (C(*C*H$_3$)$_2$). HRMS (ESI) m/z calcd for $C_{30}H_{36}N_4OSNa^+$ (M + Na)$^+$ 523.2502, found 523.2505.

The characterization ^{1}H NMR, ^{13}C NMR, and HR-ESI-MS data of the target compounds are shown in the SI.

Biological evaluation

Cell culture and reagents. The PC9 and H1975 cell lines were maintained in RPMI 1640 medium supplemented with 10%

fetal bovine serum (FBS) and 1% penicillin/streptomycin under the conditions of 5% CO_2 and 95% relative humidity at 37 °C.

The H1795 and PC9 cell lines were purchased from the Shanghai Cell Bank of the Chinese Academy of Sciences (Shanghai, China). Gibco RPMI-1640 was purchased from Thermo Fisher Scientific (Shanghai, China). Fetal bovine serum (FBS) was purchased from Yikesai Biotechnology (Taicang) Co., Ltd. RIPA lysis buffer and BCA protein assay kit were purchased from Beyotime (Hangzhou, China). TGF-β1 was purchased from Sino Biological (Beijing, China). Anti-E-cadherin, anti-vimentin, and β-actin antibodies were purchased from Proteintech (Wuhan, China). Anti-MMP9 antibody was purchased from Abcam (Cambridge, MA, UK). Anti-MMP2 and tubulin antibodies were purchased from ABclonal (Wuhan, China).

MTT assay

In the MTT assay, all cells were seeded in 96 well plates and 5×10^3 cells per well. After culturing overnight, various concentrations (0, 6.25, 12.5, 25, and 50 μM) of the derivatives were added to the cells and cultured for 48 h. Then, MTT solution (5 mg mL^{-1}) was added to each well and incubated at 37 °C for 4 h. The medium was removed and DMSO was added to dissolve formazan. The absorbance was measured at 490 nm using a microplate spectrophotometer (Synergy HT, BioTek, Vermont, USA).

Cell cycle analysis

Cells were seeded in 6 well plates at a concentration of 3×10^5 cells per well and incubated overnight. Following this, the cells were treated with compound **2f** and incubated for 24 h. Subsequently, the cells were digested and washed 1–2 times with pre-cooled phosphate-buffered saline (PBS). To fix the cells, 1 mL of 70% ethanol solution was added, and the samples were incubated at 4 °C overnight. After fixation, the cells were centrifuged and washed again with PBS. Propidium iodide (PI) was then added for staining, and the samples were incubated at 37 °C for 30 min. The cell cycle distribution was subsequently analyzed using flow cytometry.

Transwell migration and invasion assay

The migration and invasion experiment of tumor cells was performed using Transwell chambers (24 wells, 8 μm pore size, and 6.5 mm diameter polycarbonate membranes that were coated with 1 mg per mL fibronectin). The cells were seeded onto each upper well at a concentration of 2×10^5 PC9 cells and different concentrations of compound **2f** (0, 1, 2 and 4 μM) were added. The bottom chambers of the Transwell contained 600 μL of 10% FBS medium. Then, the cells were cultured for 24 h, fixed with 4% paraformaldehyde for 30 min, and stained with crystal violet solution for 20 min. Finally, the migrating and invasive cells were recorded under a light microscope at 10× magnification.

Transwell migration and invasion with TGF-β-induced assay

The migration and invasion experiment of tumor cells was performed using Transwell chambers (24 well, 8 μm pore size, 6.5 mm diameter polycarbonate membranes that were coated with 1 mg per mL fibronectin). The cells were seeded onto each upper well at a concentration of 2×10^5 PC9 cells, treated with TGF-β (30 ng mL^{-1}), and different concentrations of compound **2f** were added. The bottom chambers of the Transwell contained 600 μL of 10% FBS medium. Then, the cells were cultured for 24 h, fixed with 4% paraformaldehyde for 30 min, and stained with crystal violet solution for 20 min. Finally, the migrating and invasive cells were recorded under a light microscope at 10× magnification.

Western blotting

Western blotting analysis was carried out as previously described.[44] PC9 cells were cultured in 6 well plates at a concentration of 3×10^6 cells. The cells were treated with TGF-β (30 ng mL^{-1}) and different concentrations of compound **2f** (0, 1, 2, and 4 μM) and incubated for 24 h. After that, the cells were washed and lysed. Proteins were extracted and quantified. Proteins were separated by SDS-PAGE and transferred to PVDF membrane. The PVDF membrane was blocked with 5% non-fat milk and incubated with primary antibodies (E-cadherin, vimentin, MMP-2 and MMP-9) at 4 °C overnight. After washing with Tris-buffered saline/Tween 20 buffer, the PVDF membranes were incubated with the secondary antibodies for 2 h at room temperature. Finally, protein bands were recorded using a chemiluminescent gel imaging system (Bio-Rad, Hercules, CA, USA). Anti-tubulin and anti-β-actin were used as internal controls.

In vivo antitumor efficacy

Female Balb/c nude mouse (16–20 g) around four weeks old were purchased from Qinglongshan Biotechnology (Jiangsu) Co., Ltd. All mouse experiments were approved by the Ethical Committee of Bengbu Medical University (IACUC BBMU 2023-166). Estrogen has been demonstrated to play a promotive role in the tumorigenesis and progression of NSCLC. Given that PC9 cells exhibit significantly higher tumour formation rates in female nude mice compared to males, we employed female Balb/c nude mice for the evaluation of *in vivo* antitumor efficacy in this study.[45] We evaluated the *in vivo* anticancer efficacy of compound **2f** using a non-small cell lung cancer xenograft model. Tumour-bearing mice were randomly divided into three groups ($n = 5$/group) when the size of the tumour reached about 100 mm^3. The mice in different groups were intraperitoneally injected with saline, DDP (2 mg kg^{-1}), and compound **2f** (20 mg kg^{-1}) every 3 days. At approximately day 18, the average tumour volume reached 1000 mm^3 and the experiment was terminated. The body weight and tumour volume were monitored every three days. The size of the tumour was calculated using the following formula: volume of tumour $= 1/2 \times \text{width}^2 \times \text{length}$. All mice were anaesthetised with isoflurane and sacrificed on the final day of therapy through cervical dislocation. The

tumours in different groups were harvested for measuring their size. Additionally, the organs (heart, liver, spleen, lung, and kidney) were harvested for the evaluation of organ injury in nude mice by staining with H&E and imaged.

Immunohistochemistry assay

The expression of E-cadherin and vimentin in the mouse tumour tissues was evaluated by immunohistochemistry (IHC). The tumour tissues in each group were isolated and fixed with 4% paraformaldehyde.

Statistical analysis

All data were analyzed using GraphPad Prism software version 8.0 and expressed as the mean ± SD from three independent experiments. The Student's *t*-test was used for statistical comparison between two groups. $^{*}p < 0.05$, $^{**}p < 0.01$, $^{\#\#}p < 0.01$ and $^{***}p < 0.001$ were considered statistically significant.

Author contributions

Meng-Fan Xu contributed to the synthesis of compounds, *in vitro* experiments, western blot and data curation. Ke Zhong and Jing Zhu contributed to the *in vivo* experiments and western blotting. Jie Chen contributed to the experimental methodology, synthesis of compounds and data analysis. Fang Liu contributed to the funding acquisition, resources, guidance and supervision of the *in vivo* experiments. Feng Ding contributed to the experimental design and supervision of the *in vitro* experiment. Cheng-Zhu Wu and Long Zhao contributed to the conceptualization, supervision, funding acquisition and writing. All authors approved the final version of the manuscript and are responsible for all aspects of the work.

Conflicts of interest

The authors report no conflicts of interest.

Data availability

The data supporting this article have been included as part of the supplementary information (SI). Supplementary information is available. See DOI: **https://doi.org/10.1039/d5ra04625d**.

Acknowledgements

This work was financially supported by the Foundation of Bengbu Medical College (2022byzd013), the 512 Talent Cultivation Plan of Bengbu Medical College (By51202202); and the Natural Science Research Project of the Education Department of Anhui, China (KJ2021A0788).

Notes and references

1 J. Yang, P. Antin, G. Berx, C. Blanpain, T. Brabletz, M. Bronner, K. Campbell, A. Cano, J. Casanova, G. Christofori, S. Dedhar, R. Derynck, H. L. Ford, J. Fuxe, A. G. Herreros, G. J. Goodall, A. Hadjantonakis, R. J. Y. Huang, C. Kalcheim, R. Kalluri, Y. B. Kang, Y. Khew-Goodall, H. Levine, J. S. Liu, G. D. Longmore, S. A. Mani, J. Massagué, R. Mayor, D. McClay, K. E. Mostov, D. F. Newgreen, M. A. Nieto, A. Puisieux, R. Runyan, P. Savagner, B. Stanger, M. P. Stemmler, Y. Takahashi, M. Takeichi, E. Theveneau, J. P. Thiery, E. W. Thompson, R. A. Weinberg, E. D. Williams, J. H. Xing, B. H. P. Zhou, G. J. Sheng and EMT International Association (TEMTIA), *Nat. Rev. Mol. Cell Biol.*, 2020, **21**, 341.
2 R. Fontana, A. Mestre-Farrera and J. Yang, *Annu. Rev. Pathol.*, 2024, **19**, 133.
3 Y. H. Huang, W. Q. Hong and X. W. Wei, *J. Hematol. Oncol.*, 2022, **15**, 129.
4 H. L. Ang, C. D. Mohan, M. K Shanmugam, H. C. Leong, P. Makvandi, K. S. Rangappa, A. Bishayee, A. P. Kumar and G. Sethi, *Med. Res. Rev.*, 2023, **43**, 1141.
5 S. Brabletz, H. Schuhwerk, T. Brabletz and M. P. Stemmler, *EMBO J.*, 2021, **40**, e108647.
6 P. Debnath, R. S. Huirem, P. Dutta and S. Palchaudhuri, *Biosci. Rep.*, 2022, **42**, BSR20211754.
7 D. D. Li, L. Y. Xia, P. Huang, Z. D. Wang, Q. W. Guo, C. C. Huang, W. D. Leng and S. S. Qin, *Cell Prolif.*, 2023, **56**, e13423.
8 N. Ebrahimi, M. S. Manavi, F. Faghihkhorasani, S. S. Fakhr, F. J. Baei, F. F. Khorasani, M. M. Zare, N. P. Far, F. Rezaei-Tazangi, J. Ren, R. J. Reiter, N. Nabavi, A. R. Aref, C. Chen, Y. N. Ertas and Q. Lu, *Cancer Metastasis Rev.*, 2024, **43**, 457.
9 S. K. Jha, G. D. Rubis, S. R. Devkota, Y. L. Zhang, R. Adhikari, L. A. Jha, K. Bhattacharya, S. Mehndiratta, G. Gupta, S. K. Singh, N. Panth, K. Dua, P. M. Hansbro and K. R. Paudel, *Ageing Res. Rev.*, 2024, **97**, 102315.
10 P. X. Chen, Y. H. Liu, Y. K. Wen and C. C. Zhou, *Cancer Commun.*, 2022, **42**, 937.
11 R. L. Siegel, K. D. Miller, H. E. Fuchs and A. Jemal, *Ca-Cancer J. Clin.*, 2022, **72**, 7.
12 S. D. Deas, N. Huprikar and A. Skabelund, *Curr. Opin. Pulm. Med.*, 2017, **23**, 167.
13 R. Manshouri, E. Coyaud, S. T. Kundu, D. H. Peng, S. A. Stratton, K. Alton, R. Bajaj, J. J. Fradette, R. Minelli, M. D. Peoples, A. Carugo, F. J. Chen, C. Bristow, J. J. Kovacs, M. C. Barton, T. Heffernan, C. J. Creighton, B. Raught and D. L. Gibbons, *Nat. Commun.*, 2019, **10**, 5125.
14 Y. X. Li, C. Sun, Y. G. Tan, H. Y. Zhang, Y. C. Li and H. W. Zou, *Int. J. Biol. Sci.*, 2021, **17**, 635.
15 Z. Chen, K. Jin, L. Y. Gao, G. D. Lou, Y. Jin, Y. P. Yu and Y. J. Lou, *Eur. J. Pharmacol.*, 2010, **643**, 170.
16 D. E. Lee, E. H. Jang, C. Bang, G. L. Kim, S. Y. Yoon, D. H. Lee, J. Koo, J. H. Na, S. Lee and J. H. Kim, *Arch. Biochem. Biophys.*, 2021, **709**, 108969.
17 M. X. Lin, Q. Xu, Y. Luo, G. H. Liu and P. F. Hou, *J. Biochem. Mol. Toxicol.*, 2023, **37**, e23401.
18 R. Majeed, M. V. Reddy, P. K. Chinthakindi, P. L. Sangwan, A. Hamid, G. Chashoo, A. K. Saxena and S. Koul, *Eur. J. Med. Chem.*, 2012, **49**, 55.

19 A. Kumar, G. Sawhney, R. K. Nagar, N. Chauhan, N. Gupta, A. Kaul, Z. Ahmed, P. Sangwan, P. S. Kumar and G. Yadav, *Int. Immunopharmacol.*, 2021, **91**, 107264.
20 H. B. Yao, H. S. Almoallim, S. A. Alharbi and H. Feng, *Appl. Biochem. Biotechnol.*, 2024, **196**, 3456.
21 H. X. Liu, W. Guo, H. Guo, L. Zhao, L. Yue, X. Li, D. Y. Feng, J. N. Luo, X. Wu, W. X. Cui and Y. Qu, *Front. Pharmacol*, 2020, **11**, 712.
22 A. Cariola, M. E. Chami, J. Granatieri and L. Valgimigli, *Food Chem.*, 2023, **405**, 134953.
23 H. Mehmood, M. Musa, S. Woodward, M. S. Hossan, T. D. Bradshaw, M. Haroon, A. Nortcliffe and T. Akhtar, *RSC Adv.*, 2022, **12**, 34126.
24 X. Zhao and D. R. Richardson, *Biochim. Biophys. Acta, Rev. Cancer*, 2023, **1878**, 188871.
25 X. H. Jiang, L. A. Fielding, H. Davis, W. Carroll, E. C. Lisic and J. E. Deweese, *Int. J. Mol. Sci.*, 2023, **24**, 12010.
26 J. Kopecka, A. Barbanente, D. Vitone, F. Arnesano, N. Margiotta, P. Berchialla, M. Niso, C. Riganti and C. Abate, *Pharmacol. Rep.*, 2023, **75**, 1588.
27 P. Heffeter, V. F. S. Pape, É. A. Enyedy, B. K. Keppler, G. Szakacs and C. R. Kowol, *Antioxid. Redox Signaling*, 2019, **30**, 1062.
28 O. Farsa, V. Ballayová, R. Žáčková, P. Kollar, T. Kauerová and P. Zubáč, *Int. J. Mol. Sci.*, 2022, **23**, 9813.
29 X. G. Bai, Y. Y. Zheng and J. X. Qi, *Front. Pharmacol*, 2022, **13**, 1018951.
30 F. Miglioli, M. D. Franco, J. Bartoli, M. Scaccaglia, G. Pelosi, C. Marzano, D. Rogolino, V. Gandin and M. Carcelli, *Eur. J. Med. Chem.*, 2024, **276**, 116697.
31 V. Pape, S. Tóth, A. Füredi, K. Szebényi, A. Lovrics, P. Szabó, M. Wiese and G. Szakács, *Eur. J. Med. Chem.*, 2016, **117**, 335.
32 B. Hu, B. Wang, B. Zhao, Q. Guo, Z. H. Li, X. H. Zhang, G. Y. Liu, Y. Liu, Y. Tang, F. Luo, Y. Du, Y. X. Chen, L. Y. Ma and H. M. Liu, *MedChemComm*, 2017, **8**, 2173–2180.
33 D. Lane, T. Mills, N. Shafie, A. Merlot, R. S. Moussa, D. Kalinowski, Z. Kovacevic and D. Richardson, *Biochim. Biophys. Acta*, 2014, **1845**, 166–181.
34 X. H. Zhang, B. Wang, Y. Y. Tao, Q. Ma, H. J. Wang, Z. X. He, H. P. Wu, Y. H. Li, B. Zhao, L. Y. Ma and H. M. Liu, *Eur. J. Med. Chem.*, 2020, **199**, 112349.
35 J. Yang, L. J. Wang, J. J. Liu, L. Zhong, R. L. Zheng, Y. Xu, P. Ji, C. H. Zhang, W. J. Wang, X. D. Ling, L. L. Li, Y. Q. Wen and S. Y. Yang, *J. Med. Chem.*, 2012, **55**, 10685–10699.
36 C. J. Xu, Y. F. Han, S. C. Xu, R. X. Wang, M. Yue, Y. Tian, X. F. Li, Y. F. Zhao and P. Gong, *Eur. J. Med. Chem.*, 2020, **186**, 111867.
37 B. C. Bade and C. S. D. Cruz, *Clin. Chest Med.*, 2020, **41**, 1.
38 S. Krieg, S. I. Fernandes, C. Kolliopoulos, M. Liu and S. M. Fendt, *Cancer Discov.*, 2024, **14**, 934.
39 N. Johansson, M. Ahonen and V. M. Kähäri, *Cell. Mol. Life Sci.*, 2000, **57**, 5.
40 T. Nagai, T. Ishikawa, Y. Minami and M. Nishita, *J. Biochem.*, 2020, **167**, 347.
41 V. Aggarwal, C. A. Montoya, V. S. Donnenberg and S. Sant, *iScience*, 2021, **24**, 102113.
42 H. Schuhwerk and T. Brabletz, *Semin. Cancer Biol.*, 2023, **97**, 86.
43 J. H. Lee and J. Massagué, *Semin. Cancer Biol.*, 2022, **86**, 136.
44 J. Chen, L. Zhao, M. F. Xu, D. Huang, X. L. Sun, Y. X. Zhang, H. M. Li and C. Z. Wu, *J. Enzym. Inhib.*, 2024, **39**, 2292006.
45 N. Svoronos, A. Perales-Puchalt, M. J. Allegrezza, M. R. Rutkowski, K. K. Payne, A. J. Tesone, J. M. Nguyen, T. J. Curiel, M. G. Cadungog, S. Singhal, E. B. Eruslanov, P. Zhang, J. Tchou, R. Zhang and J. R. Conejo-Garcia, *Cancer Discov.*, 2017, **7**, 72–85.